

The crop residue conundrum: maintaining long-term soil organic carbon stocks while reinforcing the bioeconomy, compatible endeavors?

Christhel Andrade (✉ andraded@insa-toulouse.fr)

1 Toulouse Biotechnology Institute (TBI), INSA, INRAE UMR792, and CNRS UMR5504, Federal University of Toulouse, 135 Avenue de Ranguueil, F-31077, Toulouse, France. 2 Department of Chemical, Biotechnological and Food Processes, Faculty of Mathematical, Physics and Chemistry Sciences. Universidad Técnica de Manabí (UTM), 130150 Portoviejo, Ecuador. <https://orcid.org/0000-0002-2448-6186>

Hugues Clivot

3 Université de Reims Champagne Ardenne, INRAE, FARE, UMR A 614, 51097 Reims, France.

Ariane Albers

1 Toulouse Biotechnology Institute (TBI), INSA, INRAE UMR792, and CNRS UMR5504, Federal University of Toulouse, 135 Avenue de Ranguueil, F-31077, Toulouse, France.

Ezequiel Zamora-Ledezma

4 Faculty of Agriculture Engineering. Universidad Técnica de Manabí (UTM), 13132 Lodana, Ecuador.

Lorie Hamelin

1 Toulouse Biotechnology Institute (TBI), INSA, INRAE UMR792, and CNRS UMR5504, Federal University of Toulouse, 135 Avenue de Ranguueil, F-31077, Toulouse, France.

Research Article

Keywords: bioeconomy, SOC modeling, crop residues, recalcitrance, biochar, hydrochar, bioethanol molasses, digestate

Posted Date: March 18th, 2022

DOI: <https://doi.org/10.21203/rs.3.rs-1447950/v2>

License:   This work is licensed under a Creative Commons Attribution 4.0 International License.

[Read Full License](#)

1 **The crop residue conundrum: maintaining long-term soil organic carbon stocks**
2 **while reinforcing the bioeconomy, compatible endeavors?**

3 Christhel Andrade^{1,2*}, Hugues Clivot³, Ariane Albers¹, Ezequiel Zamora-Ledezma⁴,
4 Lorie Hamelin¹

5 ¹ Toulouse Biotechnology Institute (TBI), INSA, INRAE UMR792, and CNRS
6 UMR5504, Federal University of Toulouse, 135 Avenue de Ranguel, F-31077,
7 Toulouse, France.

8 ² Department of Chemical, Biotechnological and Food Processes, Faculty of
9 Mathematical, Physics and Chemistry Sciences. Universidad Técnica de Manabí
10 (UTM), 130150 Portoviejo, Ecuador.

11 ³ Université de Reims Champagne Ardenne, INRAE, FARE, UMR A 614, 51097
12 Reims, France.

13 ⁴ Faculty of Agriculture Engineering. Universidad Técnica de Manabí (UTM), 13132
14 Lodana, Ecuador.

15 *Corresponding author: andraded@insa-toulouse.fr . ORCID: 0000-0002-2448-6186

16 **ABSTRACT**

17 Crop residues are key for supplying carbon to the bioeconomy without interfering with
18 food security. However, it is often suggested to export no more than half of this
19 potential to ensure the maintenance of soil organic carbon (SOC) stocks. In this study,
20 we challenge this idea by assessing how the residues usage for the bioeconomy is
21 intertwined with the maintenance of long-term SOC stocks and thus the amount that can
22 safely be harvested. We considered the coproduct return to the soil from five
23 bioeconomy scenarios: i) pyrolysis biochar, ii) gasification biochar, iii) hydrothermal

24 liquefaction hydrochar, iv) anaerobic digestion digestate, and v) lignocellulosic ethanol
25 molasses. To compare the long-term SOC changes from these scenarios against a
26 business-as-usual (BAU) scenario, in which crop residues are unharvested, we
27 developed a framework coupling a SOC model with a bioeconomy module, that we
28 applied at high spatial resolution to cover over 60,000 combinations of crop rotations
29 and pedoclimatic units over France, for 2020 – 2120. The adapted SOC model considers
30 the recalcitrance to degradation of each coproduct, while the bioeconomy module
31 determines the share of carbon from the crop residues allocated to the coproducts. Our
32 results show that the available harvestable crop residues could be completely harvested
33 if pyrolysis or gasification biochar returns to soils, with SOC expected to double
34 compared to the BAU scenario. Replacing crop residues with hydrochar showed
35 increased SOC stocks in 88% of the areas (max +8%), while the digestate scenario
36 predicted minor SOC increases in 50% (max +0.76%) and decreases in 40% of the areas
37 (min -4%). The molasses scenario yielded SOC losses in all the areas and is thus not
38 recommended. Excluding these, an additional amount of 60.4 – 191 PJ of crop residues
39 (use-dependent) could be available for the French bioeconomy compared to applying a
40 universal removal rate of 31.5%.

41 **Key words:** bioeconomy, SOC modeling, crop residues, recalcitrance, biochar,
42 hydrochar, bioethanol molasses, digestate

43 **1. INTRODUCTION**

44 Crop residues are a key feedstock to supply non-fossil carbon (C) to the future
45 bioeconomy. In Europe alone, a theoretical potential of 3800 PJ y⁻¹ (Hamelin et al.,
46 2019) was estimated; equivalent to the gross annual electricity generation of France and
47 Germany combined (BP, 2021). Crop residues include a variety of streams, such as (i)
48 dry stalks and leaves of cereal and (ii) oilseed crops, and (iii) stems and leaves from

49 tubers. These streams are leftover from harvest operations and thus not a primary
50 economic product (Karan and Hamelin, 2021). This biomass is key for the bioeconomy,
51 as it is widely available in large quantities, at low costs, and with short harvest times,
52 besides not directly competing with food security (Sadh et al., 2018; Swain et al., 2019).
53 Current uses of crop residues include animal fodder and bedding, mushroom
54 production, mulch to preserve soil moisture, among others (Hamelin et al., 2019; Scarlat
55 et al., 2019).

56 When left unharvested, crop residues can contribute to soil organic carbon (SOC) and
57 play a key role in the long-term quality, nutrient balance, and agronomic functions of
58 soils. Increasing removal rates reduce the soil organic matter inputs, which creates a
59 tradeoff between the crop residue use for the bioeconomy and SOC stocks maintenance
60 (Blanco-Canqui, 2013; Morais et al., 2019).

61 Various studies suggested limiting the removal to rates between 15% and 60% of the
62 theoretical harvesting potential (depending on the crop type) due to technical and
63 environmental constraints (Fischer et al., 2010; Haase et al., 2016; Monforti et al., 2015;
64 Panoutsou and Kyriakos, 2021; Scarlat et al., 2019). These restrictions significantly
65 reduce the supply of renewable carbon from crop residues to the bioeconomy.

66 Bioeconomy processes convert biomass into a main product, while the more
67 degradation-resistant fraction remains a coproduct. Coproducts can be applied to the
68 soils as exogenous organic matter (EOM) to maintain or improve the SOC stocks
69 (Cayuela et al., 2010). EOM is a heterogeneous material and can be composed of
70 recalcitrant and labile fractions. The labile fractions tend to be mineralized fast (i.e., as
71 CO₂ emissions) after the first couple of years following soil application, while the
72 recalcitrant fractions exhibit longer mean residence times (MRT; (Lehmann et al.,
73 2015)), promoting SOC storage (Bera et al., 2019; Lehmann et al., 2015). SOC stock

74 evolution depends on the applied coproduct as well as the site-specific conditions and
75 cropping systems (i.e., a combination of soil properties, climate, crop rotations, and
76 other management practices). Spatially explicit considerations are thus needed in order
77 to address the conundrum between long-term SOC storage and the supply of a
78 renewable C feedstock to the bioeconomy.

79 Some soil C models can simulate long-term SOC dynamics considering different
80 cropping systems and climates (Smith et al., 2020). Organic matter decomposition
81 involves complex processes influenced by the biomass characteristics, eventual
82 stabilization treatment and/or recalcitrance degree, pedoclimatic conditions, and
83 interactions with the soil microbiota, among others. An accurate prediction of the
84 coproducts' carbon persistence in soils is therefore challenging (Lehmann et al., 2020;
85 Mondini et al., 2017). Some soil models have been adapted, or parameters have been
86 proposed to simulate the return of bioeconomy coproducts into soils. This includes, for
87 instance, RothC (Lefebvre et al., 2020; Woolf and Lehmann, 2012), Century (Dil and
88 Oelberman), APSIM (Archontoulis et al., 2016), and EPIC (Lyckuk et al., 2015) for
89 biochar; CTOOL (Hansen et al., 2020), AMG (Levavasseur et al., 2020), CANDY
90 (Witing et al., 2018), and RothC (Mondini et al., 2017) for digestate. RothC (Mondini et
91 al., 2017) has also been adapted to consider bioethanol coproducts, such as the non-
92 fermentable residue. BioEsoil, a RothC based tool, evaluates the effect of residues from
93 bioenergy processes (i.e., gasification and incineration) on soil organic matter (Bonten
94 et al., 2014). However, these studies have been location- and coproduct-specific, limited
95 to very specific simulation parcels due to the scarcity of data and modeling issues to
96 cover high spatial resolutions and temporal scales. To date, only a few studies have used
97 a soil model that includes different EOM inputs coupled with large-scale spatial

98 information, as in Mondini et al. (2018), where eight types of EOMs were simulated at
99 the scale of entire Italy.

100 The effect of crop residues harvesting and their use in the bioeconomy on long-term
101 SOC stocks has been explored in Hansen et al. (2020), where the authors found that as
102 an average for Danish soils, the straw that can be harvested for pathways involving no C
103 return is 26% of what can be harvested if the digestate is returned to soils. Yet, Hansen
104 et al. (2020) assessed only one bioeconomy conversion pathway and used a rather
105 coarse spatial representation of Danish croplands limited to two types of crop rotations
106 and three types of soils. Similarly, Woolf and Lehmann (2012) predicted that applying
107 biochar to soils could increase SOC stocks by 30–60% in 100 years while removing
108 50% of crop residues for bioenergy in three specific locations in Colombia, Kenya, and
109 the USA.

110 To our knowledge, no study has addressed the effect on SOC stocks from crop residue
111 removal and C return to the soil from various bioeconomy conversion pathways. In this
112 work, we challenge the idea that the biomass potential from crop residues must be
113 limited by a given removal rate, to maintain organic carbon in arable soils. Instead, we
114 propose that such potential is deeply intertwined with the use of the biomass within the
115 bioeconomy. This is based on the rationale that many technologies involve a potential
116 carbon return to soils as a coproduct more recalcitrant to degradation than the original
117 raw biomass.

118 Thus, this study aims to (i) further understand the cause-effect link between the “C-
119 neutral harvest” of crop residues (defined below) and their usage within the
120 bioeconomy, and (ii) address how this differs among the major existing bioeconomy
121 pathways where a C return to the soil is possible. To this end, we modeled, as an
122 illustrative case study, the SOC evolution of all arable topsoils (0–30 cm) in France,

123 with and without crop residues harvest for different bioeconomy pathways. The term
124 “C-neutral harvest” is herein employed to designate situations where the long-term
125 (here defined as 100 y) SOC stocks of a given bioeconomy management do not
126 decrease, in comparison to a reference situation where crop residues are incorporated
127 into soils. It encompasses a similar vision to what previous studies referred to as
128 “sustainable harvest” (Scarlat et al., 2019) but is more explicit on what it covers
129 (quantification of SOC stocks only) and what it disregards (e.g., other aspects of long-
130 term sustainability such as biodiversity or soil fertility).

131 **2. MATERIALS AND METHODS**

132 We propose a modeling framework to assess the long-term SOC stock effects of crop
133 residues usage for different bioeconomy technologies, considering different
134 management practices on arable topsoils. It quantifies the amount of harvestable crop
135 residues that can be removed from fields for bioeconomy, while an alternative
136 coproduct is returned to meet the condition of maintaining or even increasing the SOC
137 stock levels, as compared to a reference situation where residues are left on the field.

138 The bioeconomy scenarios considered here include pyrolysis, gasification,
139 hydrothermal liquefaction (HTL), anaerobic digestion (AD), and lignocellulosic
140 bioethanol (2GEtOH) production.

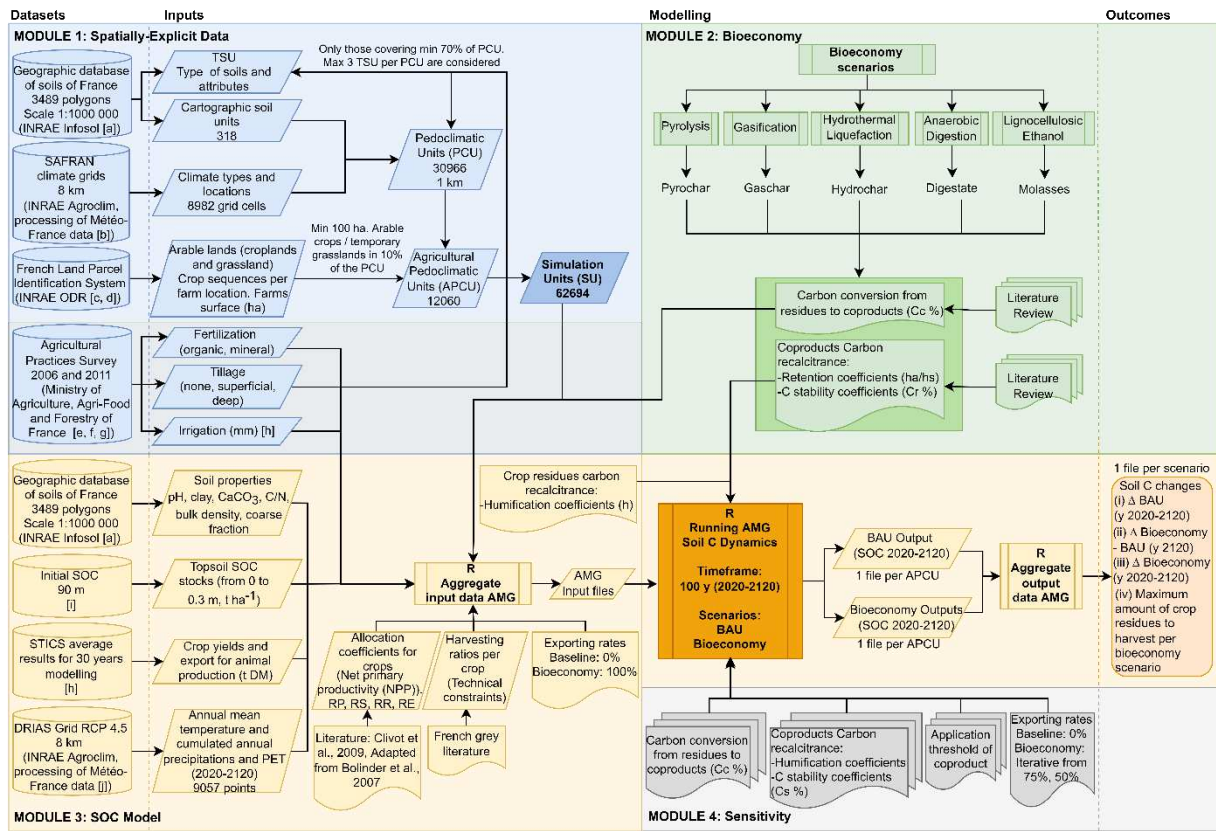
141 The framework is based on spatially explicit high-resolution data on climate, soil, and
142 agricultural practices of specific units of metropolitan France and a SOC model that
143 simulates the SOC stock changes in cropping systems receiving coproduct inputs with
144 specific recalcitrance properties. The temporal scope is 100 years, over the years 2020-
145 2120.

146 The state of C in arable soils, agricultural practices, soil, and climate at the beginning of
147 the time scope is here referred to as the initial conditions. Two developments over the
148 time scope are considered: (i) a business as usual (BAU) scenario reflecting current
149 practices where part of the harvestable crop residues (ca. 46%; details in SI1.2) are
150 already being exported for livestock (as bedding and fodder) and the rest is left on
151 fields, and (ii) a bioeconomy scenario which is similar to the BAU, except that the share
152 of straw left on fields is harvested, used in the bioeconomy (five distinct bioeconomy
153 scenarios being independently considered), and partly returned to fields as a
154 bioeconomy coproduct. The BAU scenario is thus a measure-stick against which the
155 bioeconomy scenarios are contrasted. For these six future developments (i.e., BAU and
156 the five bioeconomy scenarios), the long-term changes in SOC stocks are determined as
157 further described in section 2.3.

158 The soil physicochemical properties and the future meteorological variables assumed
159 (further detailed in sections 2.2 and 2.3) are the same for the BAU and bioeconomy
160 scenarios. Similarly, the same rotations, farming management practices (section 2.2),
161 and crop yields (SI1.2) are repeated cycle after cycle. The impact on crop yields, from
162 changing the raw biomass to stabilized EOM (Oldfield et al., 2019), was excluded to
163 emphasize the effect of crop residue removal alone. The technical harvestable rate and
164 amount of crop residues already used for livestock are crop-dependent (Table SI1.1) and
165 are assumed to remain constant during the modeling timeframe.

166 The structure of the framework consists of four main modules (Fig. 1), further detailed
167 in the subsequent subsections: description of the simulation units (Module 1), definition
168 of the bioeconomy scenarios, carbon conversion from residues to coproducts, and
169 recalcitrance of coproducts (Module 2), modeling SOC stock changes and collecting
170 related input data (Module 3), and sensitivity analysis (Module 4). The process was

171 automated using R (R Core Team, 2021); the scripts and data used are available in
 172 <https://doi.org/10.48531/JBRU.CALMIP/AUEEEJ>.



173

174 [a] Jamagne et al., 1995

175 [b] Based on Durand et al., 1993 after adaptation of Launay et al., 2021

176 [c] <https://www.geoportail.gouv.fr/donnees/registre-parcellaire-graphique-rpg-2010>

177 [d] Leenhardt et al., 2012

178 [e] <http://agreste.agriculture.gouv.fr/enquetes/pratiques-culturelles/2006>

179 [f] <http://agreste.agriculture.gouv.fr/recensement-agricole-2010/>

180 [g] Graux et al., 2020

181 [h] Launay et al., 2021

182 [i] Mulder et al., 2016

183 [j] CNRM-CERFACS-CM5--CNRM/ALADIN 63. Model GCM / RCM – correction

184 ADAMONT. Institution : Météo-France/CNRM, <http://www.drias-climat.fr/>

185 PET : Potential Evapotranspiration

186 RP: Relative Carbon allocation coefficient for the agricultural product
187 RR: Relative Carbon allocation coefficient for roots
188 RS: Relative Carbon allocation coefficient for straw or any post-harvest residue
189 RE: Relative Carbon allocation coefficient for extra root material
190 BAU: Business as Usual
191 SOC: Soil organic carbon
192 STICS: Soil-crop model used in Launay et al., (2021)
193 DRIAS: Spatially explicit database for France projections of climate scenarios
194 SAFRAN: Spatially explicit database for France climate
195 Figures legend: Cylinders: database, parallelogram: data input, rectangle: process, rectangle
196 with inner bars: process containing more processes, curved bottom rectangle: manually input
197 data sets, rounded rectangle: output

198 **Fig.1.** Spatially explicit modeling framework, as applied to France, to quantify the long-
199 term SOC difference between crop residues left on land and their harvest for five
200 distinct bioeconomy pathways, with return of the coproduct.

201 *2.1 Module 1: Spatially explicit data*

202 The aim of Module 1 is to define representative simulation units (SU) for the studied
203 case, reflecting the variety of soils, climates, crop rotations, and farming practices in a
204 spatially explicit manner.

205 Module 1 is entirely building upon the study of Launay et al. (2021), launched within
206 the frame of the French efforts within the international 4p1000 initiative (“4p1000”),
207 acknowledged as the most comprehensive and updated spatially explicit representation
208 of cropping systems in France. Launay et al. (2021) defined a set of fundamental
209 concepts briefly described as follows.

210 Pedoclimatic units (PCU) are defined as a unique combination of soil properties (coarse
211 fraction, clay content, pH, etc.) and meteorological variables (temperature,
212 precipitations, and potential evapotranspiration) (French climate and soil types are
213 specified in SI1.1). When found on arable lands, these are referred to as agricultural
214 PCU (APCU). French APCUs combine soil mapping units (1:1000,000; Jamagne et al.,
215 1995) and the French SAFRAN climate grids (8x8 km; Durand et al., 1993) with
216 identified crop rotations per PCU retrieved from the French Land Parcel Identification
217 System (Leenhardt et al., 2012; Levavasseur et al., 2015). A total of 12,060 APCUs
218 with more than 100 ha of agricultural area, where at least 10% of it has arable crops
219 and/or temporary grasslands, were identified. The selection represents 84% of the
220 French cropland.

221 The crop rotations selected in Launay et al. (2021) include 12 different crops, temporary
222 grasslands, and cover crops (further detailed in SI1.2). Winter wheat is the most
223 representative crop, providing 65% of the available residual biomass (dry matter). Crop
224 rotations cover 4.79 Mha and were judged to be a fair representation of the 18.35 Mha
225 of French arable crops and temporary grasslands in 2006-2012. Farming practices —
226 involving organic fertilization, cover crops, irrigation, tillage, and current use of crop
227 residues— were determined from a survey conducted by the Ministry of Agriculture,
228 Agri-Food, and Forestry over the period 2006-2011 (Graux et al., 2020; Lafargue,
229 2013).

230 The combination of APCUs, crop rotations, and farming practices yielded 62,694
231 simulation units (SI1.1). Further details on the crop rotation and yields are presented in
232 SI1.2.

233 *2.2 Module 2: Bioeconomy scenarios*

234 This module describes the five bioeconomy scenarios. All the bioeconomy scenarios
235 involve two key parameters to answer the research questions of this study, namely (i)
236 the amount of C from the harvested crop residues (of a given SU; Fig. 1) that will end
237 up in the coproducts returned to fields and (ii) the C recalcitrance to degradation of this
238 coproduct. The former is hereafter referred to as carbon conversion (Cc) and the latter
239 as carbon recalcitrance (Cr). The recalcitrance represents the most stable biochemical
240 fraction of organic products. Here, Cr is the fraction of the coproduct that cannot be
241 readily mineralized, and which decomposes slower than the more labile fraction of the
242 organic coproduct. The labile fraction is assumed to be entirely processed by soil
243 microorganisms within about one year. The Cc and Cr of a coproduct depend on the
244 feedstock and process conditions.

245 Thermochemical processes, such as gasification, pyrolysis, and HTL, exposing biomass
246 to elevated temperatures for long times, coproduce biochar with more aromatic
247 compounds than for low temperatures and short times, thus the former is related to high
248 degrees of recalcitrance (Han et al., 2020; He et al., 2018; Wang et al., 2016). Various
249 studies determined that the recalcitrant fraction of biochar exhibits MRTs from decades
250 to millennia (Lehmann et al., 2015; Zimmerman and Gao, 2013). HTL, which is carried
251 out at lower temperatures than pyrolysis and gasification, using relatively wet feedstock,
252 produces a less recalcitrant char than pyrolysis. Gasification, which employs higher
253 temperatures than HTL and pyrolysis, yields char with a higher degree of stability than
254 pyrolysis char.

255 In this work, we only considered the return of the char produced in each thermochemical
256 technology, and other coproducts generated (e.g., tar, ashes) are excluded. To avoid
257 confusion between the coproducts assessed in each scenario, we refer to pyrolysis,
258 gasification, and HTL char as pyrochar, gaschar, and hydrochar, respectively.

259 Biochemical processes, such as alcoholic fermentation and anaerobic digestion, are
 260 carried out using microorganisms and lower temperatures than thermochemical
 261 technologies. The outputs of AD are biogas and digestate, while alcoholic fermentation
 262 produces bioethanol and a residue that is often separated into a lignin-rich solid and a
 263 liquid fraction known as molasses. The solid coproduct is typically used for energy
 264 production. Therefore, for the biochemical pathways, we consider only digestate (from
 265 AD) and molasses (from 2GEtOH production) as EOMs. The carbon stability and soil
 266 MRT of molasses and digestate are considered lower than for chars (Table 1).

267 The Cr and Cc considered herein stem from a comprehensive compilation and data
 268 reconciliation of over 600 records from laboratory assays, field trials, and modeling
 269 experiments involving a wide variety of feedstock, including crop residues, as detailed
 270 in Andrade et al. (2022). To the extent possible, the Cc and Cr values used herein were
 271 derived from studies involving straw-like feedstock. Table 1 summarizes the Cc and Cr
 272 values considered, along with the identification of the coproduct returned to fields and
 273 the other products generated during the conversion process for each scenario. The
 274 bioeconomy conversion pathways are further described in SI1.3.

275 **Table 1.** Overview of the bioeconomy scenarios considered in the study, and
 276 implications in terms of the Cc (Carbon conversion) and Cr (Carbon recalcitrance)
 277 parameters. MRT: Mean Residence time, DM: dry matter, n/a: not applicable

Scenario	Process Conditions	Coproduct returned to soil	Other products generated ^a	Cc ^b %	Cr ^b %	MRT ^c Years	Key process reference ^h
BAU	Crops residues left on soil	None	None	n/a	n/a	n/a	(Launay et al., 2021)

	350 – 700 °C, from seconds to 2h, typically fed with a biomass DM>90%		Bio-oil, non- condensable gases	44 [34 – 54]	95 [90 – 99]	> 100	(Ippolito et al., 2020; Joseph et al., 2021; Lehmann et al., 2015)
	600-1200°C dry gasification.						(Molino et al., 2018;
Gasification	hydrothermal gasification, typically fed with a DM>90%	Gaschar	Syngas, tar, ashes	20 [14 – 25]	95 [90 – 99]	> 100	Ventura et al., 2019; Watson et al., 2018)
	180-400°C, use of K ₂ CO ₃ catalyst to enhance bio-oil production;		Bio-oil, non- condensable gases	31 [12 – 45]	83 [80 – 96]	< 26	(Malghani et al., 2015; Watson et al., 2020)
Hydrothermal Liquefaction ^f	typically fed with a DM<20%	Hydrochar					
Anaerobic ^g Digestion	Mesophilic conditions (30- 50°C). 1-3 months.	Digestate	Biogas	33 [30 – 40]	68 [58 – 77]	< 26	(Hamelin et al., 2014; Sarker et al.,

	Typically, wet digestion, with DM in the digester < 35%						2019)Zhang et al 2021
	Pretreatment, acid and enzymatic hydrolysis, fermentation <i>S. cerevisiae</i> ,						(Swain et al., 2019;
Lignocellulosi	<i>purification by distillation. The effluent is separated into a solid fraction and liquid molasses</i>	Molasses	Ethanol, solid fraction	24 [18 – 30]	45 [28 – 60]	< 26	Tonini et al., 2016;
c ethanol							Wietschel et al., 2021)

278 ^aThe main product considered to drive the investment in this bioeconomy scenario, under the specified
279 conditions, is indicated in bold; ^b Cc: C fraction of initial crop residue transferred to the co-product
280 returned to fields, Cr: C fraction of the co-product allocated to the stable biochemical fraction. The values
281 presented herein are averages from Andrade et al. (2022), based on a compilation of 124, 33, 97, 99, and
282 51 records, for pyrochar, gaschar, hydrochar, digestate, and molasses, respectively. Ranges in brackets
283 represent quartiles 1 and 3; ^c The MRT allows to define the SOC fraction of the soil model to allocate the
284 Cr fraction. The soil model used in this study considers that EOMs with MRT of the Cr fraction higher
285 than the modeling timeframe are inert, thus any coproduct with an MRT longer than 100 years is virtually
286 inert. EOMs with Cr fractions exhibiting MRT of 7 – 26 years are considered to be slowly mineralized
287 (Clivot et al., 2019) in the soil model (see section 2.3). ^dPyrolysis can be classified as fast (300 – 500°C,
288 seconds of retention time) or slow (500-700°C, minutes to hours). Slow conditions tend to favor the
289 production of biochar, whereas the fast process is optimal for bio-oil production. From an economic

290 standpoint, the pyrolysis scenario in this study aims to maximize the bio-oil yields, thus the process
291 conditions of the studies included are those of a fast process, when possible (Ippolito et al., 2020). ^e Also
292 commonly referred to as biochar. ^f The use of catalysts, specially K_2CO_3 accelerates the water gas shift
293 reaction in low temperatures HTL processes, which yields higher rates of bio-oil (targeted product) than
294 hydrochar. The use of catalysts tends to be more common (Mathanker et al., 2021), therefore, the Cc and
295 Cr values stem from such process conditions. ^g Some simulation units involve the use of manure as
296 organic fertilizer. For these, we did not consider this manure to be digested, to keep the focus on the
297 impacts from crop residues. Cc accounts only for the C from crop residues transferred to the digestate. ^h
298 Only key references mentioned, the full compilation of reviewed studies is presented in Andrade et al.
299 (2022).

300 *2.3 Module 3: SOC Model*

301 Module 3 describes the SOC model used and the adaptations considered in this study, as
302 well as how the bioeconomy scenarios have been compared with the BAU scenario.

303 *2.3.1 AMG model: Overview*

304 For both the BAU and bioeconomy scenarios, the evolution of topsoil organic C stocks
305 (0-30 cm) was simulated with the AMGv2 SOC model, detailed in Clivot et al. (2019).
306 AMG is a French SOC model, first described in Andriulo et al. (1999), which simulates
307 the carbon dynamics of agricultural topsoils at an annual timestep. The model
308 successfully predicted the changes in SOC stocks of various cropping systems under
309 different pedoclimatic conditions in France and Europe (Clivot et al., 2019; Farina et al.,
310 2020; Saffih-Hdadi and Mary, 2008) and has notably been calibrated for 26 EOM types
311 (Levavasseur et al., 2020). AMG splits the organic matter (OM) into three different
312 pools (shown as boxes in Fig. 2). The fresh OM inputs from above- (crop residues) and
313 below- (crop roots and root exudates) ground plant compartments, as well as inputs
314 from EOM (e.g., manure, bioeconomy coproducts), represent the fresh organic matter
315 (FOM) pool, which is assumed to be annually decomposed (Fig. 2a). The C in the FOM

316 pool is labeled as C_{FOM} . The proportion of C_{FOM} incorporated into the active SOC pool
317 (C_A) is determined by a retention coefficient (h). The fraction of C_{FOM} that does not
318 enter C_A ($1-h$) is mineralized as CO_2 . The C_A pool is affected by the mineralization
319 process following first-order kinetics with a k mineralization rate. The stable SOC pool
320 (C_S) sets 65% of the initial SOC by default as inert during all the simulations for sites
321 with an arable land history (Clivot et al., 2019).

322 *2.3.2 Model input data*

323 AMG minimum input data comprises crop rotations, climate, soil physicochemical
324 properties, initial SOC stocks, and farming practices (including the maximal soil tillage
325 depth, irrigation water amounts, EOM inputs, and crop residue management). Crop
326 rotation information includes annual yield, moisture content of the harvested product,
327 harvest indexes (HI), and C allocation coefficients determining the proportion of C in the
328 harvested product (RP), above-ground residues (RS), root C (RR), and extra-root C (RE)
329 (Fig. 1). It also includes the fraction of residues that can be technically harvested, per crop
330 type.

331 HI and allocation coefficients were used as set in the method proposed for calculating C
332 inputs for AMGv2 (Clivot et al., 2019), themselves adapted from Bolinder et al. (2007).
333 The technically harvestable fraction for each crop was also taken as defined in the
334 proposed method (further details in Table SI1.1) and varies from 55-91%. Meteorological
335 data comprises the mean annual air temperature and the annual water balance, the latter
336 being determined as the difference between the water inputs (accumulated precipitations
337 and irrigation) and potential evapotranspiration. In this study, the spatially explicit
338 meteorological data were retrieved, for years 2020 to 2100, from SICLIMA (DRIAS, last
339 updated May 2013), for the RCP4.5 climate trajectory (Representative Concentration
340 Pathway; IPCC, 2021), downscaled by the model CNRM-CERFACS-CM5/CNRM-

341 ALADIN63. These projections were not available beyond 2100. For the period from 2101
342 to 2120, average values from the last decade (i.e., from 2091 to 2100) were used.

343 Soil-related data include initial SOC stocks, pH, bulk density, coarse fraction, clay
344 content, C:N ratio, and CaCO₃ content. Initial SOC stocks were retrieved from Mulder et
345 al. (2016) and used as processed in Launay et al. (2021) to correspond to the APCU
346 resolution, while the other soil parameters were retrieved from Jamagne et al. (1995).

347 AMG also requires information regarding farming practices, as detailed in Module 1.

348 Default h values (FOM-dependent) given in AMG for crop residues and non-coproduct
349 EOMs (e.g., animal manure) were used (Clivot et al., 2019; Levavasseur et al., 2020),
350 while for the bioeconomy coproducts were determined individually. The actual
351 mineralization rate (k) of the active SOC pool, which depends on environmental response
352 functions, is calculated for each year and each situation as defined in Clivot et al. (2019).

353 *2.3.3 AMG adapted for bioeconomy processes*

354 We adapted the calculation method for C inputs and the model to include the C_c and C_r
355 values of pyrochar, gaschar, hydrochar, digestate, and lignocellulosic ethanol molasses.
356 The adapted version of AMG allows determining the SOC evolution of the different
357 bioeconomy scenarios by deriving retention coefficients from C_r values. The C input
358 from the coproducts is determined using the initial C in the crop residues and the C_c
359 coefficient.

360 We grouped the C_r values per coproduct as highly recalcitrant (pyrochar and gaschar) and
361 less recalcitrant (hydrochar, digestate, and molasses), to define the C retention into the
362 soil associated with each coproduct. The recalcitrance and the MRT values in Table 1
363 were used to set the h coefficient per coproduct and allocate the C among the soil pools

364 (C_A or C_S), respectively. Two retention coefficients were defined to differentiate between
365 the fraction integrating the active pool (h_a) and the stable pool (h_s).

366 For the highly recalcitrant coproducts, with MRTs longer than the modeling timeframe,
367 the Cr fraction (95%; Table 1) was considered virtually inert and was directly allocated
368 into the stable pool as h_s (Fig 2b), while the labile fraction was assumed to be entirely lost
369 as CO₂ and no h_a was considered. For the less recalcitrant coproducts hydrochar,
370 digestate, and bioethanol molasses, we assumed that the labile fraction (1-Cr; 17%, 32%,
371 and 36%, respectively) was mineralized in the first year and the remaining recalcitrant
372 fraction corresponded to h_a (here equivalent to Cr) and was fully allocated to the active
373 pool (Fig. 2a). The derived h_a coefficient for the digestate (0.68) is close to the value of
374 0.65 proposed in Levavasseur et al. (2020). No reference allowing for similar comparison
375 was found for the other studied coproducts. The adaptation of AMG for the bioeconomy
376 is further detailed in SI1.4.

377 2.3.4 AMG output analysis

378 The difference in changes of SOC stocks between a given bioeconomy scenario and the
379 BAU was determined based on Eq 1.

$$380 \quad \Delta SOC_{bio-BAU}(\%) = \frac{SOC_{fbio} - SOC_{fBAU}}{SOC_{fBAU}} \quad \text{Eq 1}$$

381 where $\Delta SOC_{bio-BAU}(\%)$ is the percent change in SOC by shifting from BAU to
382 bioeconomy, SOC_{fbio} corresponds to the SOC stocks at the end of the simulation, f ,
383 (here $f = \text{year } 100$) for the bioeconomy scenario, and SOC_{fBAU} is the SOC stocks at the
384 end of the simulation for the BAU scenario.

385 Positive values of $\Delta SOC_{bio-BAU}$ represent an increase in SOC stocks for the bioeconomy
 386 scenarios as compared to the BAU scenarios, while negative values reflect SOC losses
 387 from shifting to the bioeconomy.

388 For a given scenario (BAU or bioeconomy), the change in SOC stocks over 100 years
 389 was calculated as the final SOC stock minus the initial SOC, as shown in Eq 2.:

$$390 \quad \Delta SOC_{0-100i}(\%) = \frac{SOC_{100i} - SOC_0}{SOC_0} \quad \text{Eq 2}$$

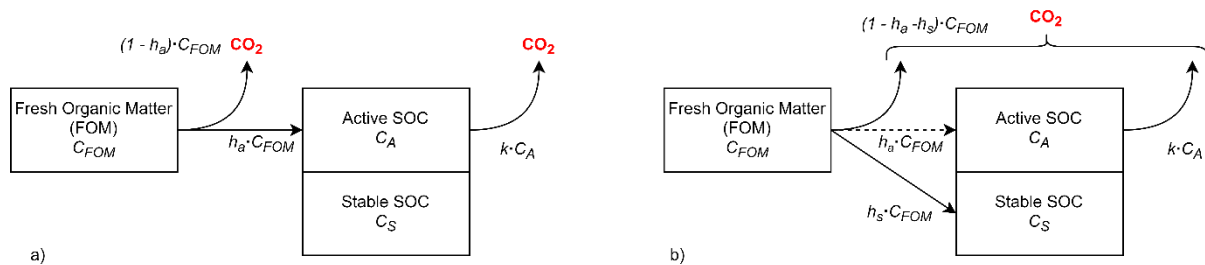
391 where $\Delta SOC_{0-100i}(\%)$ is the percent change of SOC stocks from the initial conditions
 392 (year 2020) until the end of the simulation (year 2120); SOC_0 corresponds to the initial
 393 SOC stocks and SOC_{100i} to the final SOC stocks (after 100 years), per scenario i .

394 The difference between the scenarios BAU and bioeconomy was calculated at a national
 395 scale as the total net SOC change for all the APCUs areas (Eq 3).

$$396 \quad Total\ national\ \Delta SOC_{net} = \sum_i^j (SOC_{bio} - SOC_{BAU})_j * PondCoef_{SU \times APCU_i} * S_{APCU_i}$$

397 Eq 3

398 Total national ΔSOC net (in t C) is the sum of the difference between the SOC stocks
 399 under the bioeconomy and the BAU scenarios at the year 2120 per SU, times the
 400 ponderation coefficient ($PondCoef_{SU \times APCU}$) of the SU surface in the APCU surface,
 401 times the surface of the APCU (S_{APCU}). The total APCU surface is 14.89 Mha (SI1.1)
 402 but after the selection criteria in Module 1, only 3.5 Mha were included in the SUs.
 403 $PondCoef_{SU \times APCU}$ corresponds to the weight of a SU area in each APCU and allows to
 404 scale the SOC change per SU to the APCU scale (j =identity of the SU within a given
 405 APCU, i =identity of the APCU).



406

407 **Fig. 2.** AMGv2 configuration implemented in this study (adapted from Clivot et al.,
 408 2019): a) AMG v2 (for all streams but pyro- and gaschar), and b) adaptation of AMGv2
 409 (for pyro- and gaschar). FOM: fresh organic matter, C_{FOM} : carbon in the fresh organic
 410 matter, $h_a \cdot C_{FOM}$: fraction of C_{FOM} allocated to the active pool C_A , $h_s \cdot C_{FOM}$: fraction of
 411 C_{FOM} allocated into the stable pool C_S , h_a : retention coefficient integrating a fraction of
 412 FOM into the active pool, h_s : retention coefficient integrating a fraction of FOM into the
 413 stable pool, k : mineralization rate constant, dotted line: FOM fraction allocated to the
 414 active SOC pool (see section 2.5).

415 *2.5 Module 4: Sensitivity Analysis*

416 SOC stock changes are influenced by the characteristics and amount of the carbon
 417 inputs (Keel et al., 2017). We performed a sensitivity analysis (SA) on the key
 418 parameters governing the amount of C returned to the soil contributing to SOC, namely
 419 C_c and C_r . As shown in Table 1, both C_c and C_r can vary within ranges conditioned by
 420 the process performance (itself depending on the specific process conditions) and the
 421 type of assay used to determine it (affecting C_r only). These ranges were retrieved from
 422 our review Andrade et al. (2022). Here, we use the first and third quartiles of Andrade et
 423 al. (2022) to set “low” and “high” levels for C_c and C_r for all coproducts (Table SI1.2).
 424 Combinations of low, mean, and high C_c and C_r were tested for a total of eight new sets
 425 of C_c and C_r combinations per scenario.

426 Since the long-term recalcitrance behavior of biochar is poorly understood due to a lack
427 of long-term experimental evidence in comparison to reported half-lifetimes ranging
428 from decadal- to millennial-scales (Woolf et al., 2021; Zimmerman, 2010), an
429 additional SA was performed on the procedure used to partition Cr within AMG SOC
430 pools. It was performed for the pyrolysis scenario as a representative case of a highly
431 recalcitrant EOM. In the initial method (section 2.3.3), we considered the recalcitrant
432 fraction completely inert during the simulation and fully allocated it to the C_S pool. Yet,
433 various studies suggest that the recalcitrant fraction may not be completely inert but
434 follow a very slow decay rate (Han et al., 2020; Joseph et al., 2021). Therefore, an
435 alternative partition of the recalcitrant fraction between C_A and C_S was considered. To
436 this end, we considered a remaining C fraction of 75% after 100 years, meaning that
437 25% of the initial C is mineralized during the timeframe (Andrade et al., 2022; Woolf et
438 al., 2021). From the 25%, a fraction corresponds to a very labile fraction readily
439 mineralized in the first year (4%) while the remaining corresponds to the mineralizable
440 recalcitrant fraction which is allocated to the C_A pool to be slowly mineralized. More
441 details are provided in SI1.5. The values for pyrochar covered those found in the
442 literature and suggested by the IPCC (2019), which proposes that around 80% of C in
443 biochar remains after 100 years for pyrolysis temperatures of 450-600°C. Table SI1.2
444 summarizes all the combinations explored for the SA.

445 An excessive application of biochar may be toxic for soil microbiota, which may reduce
446 plant growth (Joseph et al., 2021) and increase CH₄ and CO₂ emissions (Zhang et al.,
447 2020). To avoid this negative effect, a last SA was performed to explore the effects of
448 exporting all the available harvestable crop residues followed by the return of a lower
449 amount of coproduct than the generated. Accordingly, an extra scenario was modeled,
450 limiting the soil application rate of pyro- and gaschar to not exceed a total of 50 Mg C

451 ha⁻¹ regularly applied over 100 years, as suggested by Woolf et al. (2010) to allow char
452 storage in the soil and ensure positive or neutral effects on plant yields. The analysis of
453 alternative storage options for the portion of char not returned to the soil is out of the
454 scope of this work.

455 Finally, for occurrences where $\Delta\text{SOC}_{\text{bio-BAU}}$ (Equation 1) was negative, the portion of
456 retrieved residues from fields was decreased in steps of 25% from its initial 100% value
457 until 0%. These iterations were performed only for scenarios showing negative
458 $\Delta\text{SOC}_{\text{bio-BAU}}$ to identify possible compromises between bioeconomy exports and SOC
459 maintenance.

460 **3. RESULTS**

461 *3.1 BAU scenario*

462 The BAU scenario predicted a potential decrease of the topsoil SOC stocks by a mean
463 of 2% (Table 2) in the APCUs over 100 years, which represents a C loss of 18 Mt C at
464 the French national scale. Approximately 63% of the simulated areas predicted SOC
465 stocks decrease over 100 years, with a maximum decrease of 27% in some APCUs.
466 APCUs with SOC stock increases may raise their levels by up to 85%, mainly in the
467 Central and Western regions (Fig 3).

468 *3.2 Bioeconomy scenarios: 100% export over 100 years*

469 Crop residues are already exported for other services in 10% of the areas, making them
470 unavailable for the bioeconomy. Therefore, these areas did not present any change in
471 the bioeconomy scenarios as compared to the BAU scenario. At the national level, the
472 SOC building-up potential over 100 years of each bioeconomy scenario varies greatly;
473 it ranges from -34.9 (molasses) to 774.2 Mt C (pyrochar) (Table 2), a 22-fold difference,
474 reflecting the importance of the coproducts' C_c and C_r parameters, among others.

475 The highest additional SOC storage, as compared to the BAU, was observed for
476 pyrochar application (+105.5%), while the highest SOC loss was associated with
477 molasses return (-4.4%) (Table 2). It should be highlighted, however, that these
478 decreases and increases are highly variable across the country (Fig. 4), reflecting the
479 large variety of underlying pedoclimatic conditions and cropping practices. This applies
480 to both the BAU (Fig. 3) and bioeconomy scenarios (Fig. 4). Among others, the
481 Southwest of France tends to exhibit the largest SOC changes (both positive and
482 negative) among the different scenarios, while the SOC changes in the Northwest tend
483 to be lower (Fig 4).

484 The pyrolysis and gasification scenarios predicted enhanced SOC levels in all the
485 APCUs after 100 years, with the highest potential for SOC sequestration in the
486 Southwestern and Central regions (Fig. 4. a,c). For pyrolysis, SOC stocks increased by
487 over 100% in 57% of the country (Table S2.1), with a national mean SOC stock
488 increase of 105% (+774 Mt C, Table 2). For the gasification scenario, a mean national
489 increase of 43% (+316 Mt C, Table 2) was expected. In 85% of the modeled areas, the
490 consecutive application of gaschar could potentially increase SOC stocks by
491 approximately 80%, as compared to the BAU (max +178%) (Table S2.1; Table S2.4).

492 The return of hydrochar is shown to ensure SOC sequestration in 88% of the areas
493 (Table S2.4), with a maximum increase of 4%. At a national scale, this scenario
494 represents an average SOC change of 1.1% and a total additional C storage of 8.9 Mt C
495 (Table 2). Unlike pyrolysis and gasification, this scenario indicates potential C losses
496 (up to -1.8%). Digestate may contribute to building up SOC stocks in the North-Central
497 area of France, with predicted losses in the Southwestern and Northern regions. With
498 digestate, SOC stocks are shown to slightly increase (max 0.8%) in 50% of the
499 simulated areas (Table 2). Despite the potential SOC storage in this scenario, a mean

500 loss of 0.1% in SOC stocks is expected at a national scale over the timeframe compared
501 to the BAU scenario. For the molasses, the expected SOC stocks after 100 years are
502 lower than in the BAU scenario by a mean of 4.4% at a national scale, representing a
503 potential SOC loss of 35 Mt C (Table 2). The results indicate relative SOC reductions
504 up to 14%, with the highest losses in the Southwest, Northern, and Northeast regions.
505 For the scenarios depicting SOC losses (i.e., HTL, AD, and 2GEtOH), exporting rates
506 were re-adjusted (75%, 50%). Decreases in the export rates did not influence the overall
507 percentage of areas affected (Table S2.1), thus no lower exporting values were
508 tested. However, the export rate reduction resulted in a lower national SOC loss
509 compared with the 100% export rate for all the remodeled scenarios (Table S2.2).

510 *3.3 Sensitivity Analysis*

511 The SA allowed to evaluate the uncertainty of the potential national SOC changes at the
512 year 2120 due to variability of the Cc and Cr coefficients relative to the mean
513 coefficient value (Fig. 5).

514 For the pyrolysis scenario, the different combinations of Cc and Cr coefficients affected
515 the additional SOC stocks, ranging between -29% and +30%, equivalent to 549 Mt C
516 and 1009 Mt C (Table S2.3), at a national level. A one-at-a-time test showed the SOC
517 results to be more sensitive to Cc, ranging between -25% and +25%, while Cr ranged
518 between -6% and +5%.

519 The additional SOC stocks for all the SA tested in the gasification scenario varied by -
520 40% to +36% from that obtained using the mean coefficients, equivalent to 187-431 Mt
521 C. Cr variability contributed to SOC changes between -6% and +5%, while Cc alone
522 affected the results from -36% to +30%. From these results, it is observed that Cc has

523 the greatest influence on the pyrolysis and gasification scenario, one reason being the
524 greater range of values compared to Cr (Fig.S4, Fig.S6).

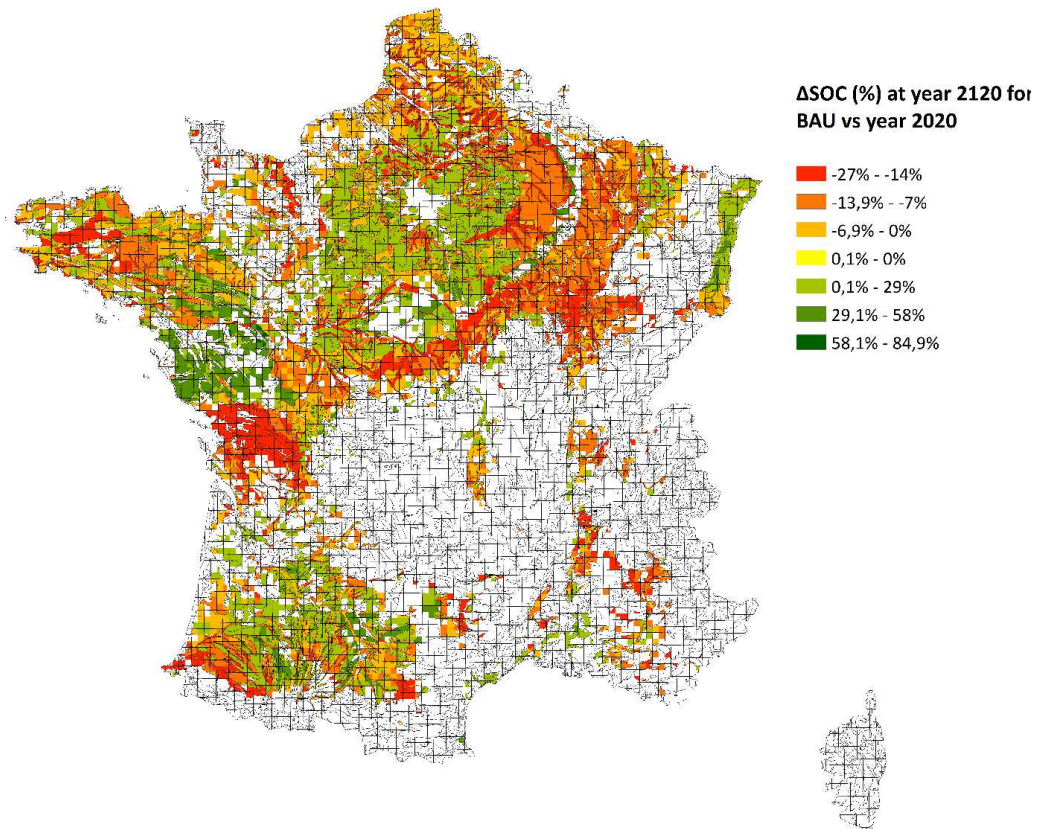
525 For the low recalcitrance scenarios, the uncertainty of the coefficients caused results to
526 vary from C losses to potential additional C storage. The HTL scenario result is affected
527 by -4.8% to +7.6%. High Cc values for any given Cr predict C sequestration in areas
528 that would potentially lose SOC stocks with the mean coefficients. The opposite was
529 observed for low Cc values, which resulted in SOC losses for all the APCUs (Fig. S7).
530 Due to the diverse possible conditions of the HTL technology, the Cc coefficients in this
531 scenario were tested for a broader range (0.12-0.45), which produced a higher effect for
532 Cc than for Cr.

533 The national SOC change ranges from -16 MtC to +24 MtC for the different
534 coefficients in the AD scenario, representing changes of -2 to 3%. The combination of
535 high Cc and Cr resulted in SOC losses in only 0.2% of the simulated areas, compared to
536 40% for the mean values of the parameters (Table S2.1). Similarly, lower Cc and Cr
537 values result in SOC stocks decreasing in all the areas (Fig S8). For the molasses
538 scenario, the combination of maximum and minimum values of Cc and Cr represented a
539 SOC stocks variation of -61% to 48% (Table S2.3) from the values obtained for the
540 mean parameters, with losses observed in all the APCUs.

541 The Cr partitioning between the C_A and the C_S pools of AMG (Pyrolysis 2) resulted in
542 cumulated additional SOC stocks of 617 Mt C compared to the BAU scenario by the
543 year 2120 (Table S2.2). This represents a difference of -21% in comparison to a 100%
544 C allocation of the recalcitrant pyrochar to the C_S pool only, with variabilities in the
545 SOC stock results ranging from -39% to -10% for all the SA coefficient combinations
546 (Table S2.3). Albeit the net additional C stored differed for the two Cr allocation
547 methods, the trend observed was the same, with expected SOC increases in all the

548 APCUs. For the Pyrolysis 2 scenario, 36% of the areas predicted SOC increases above
549 100% (Fig. S5).

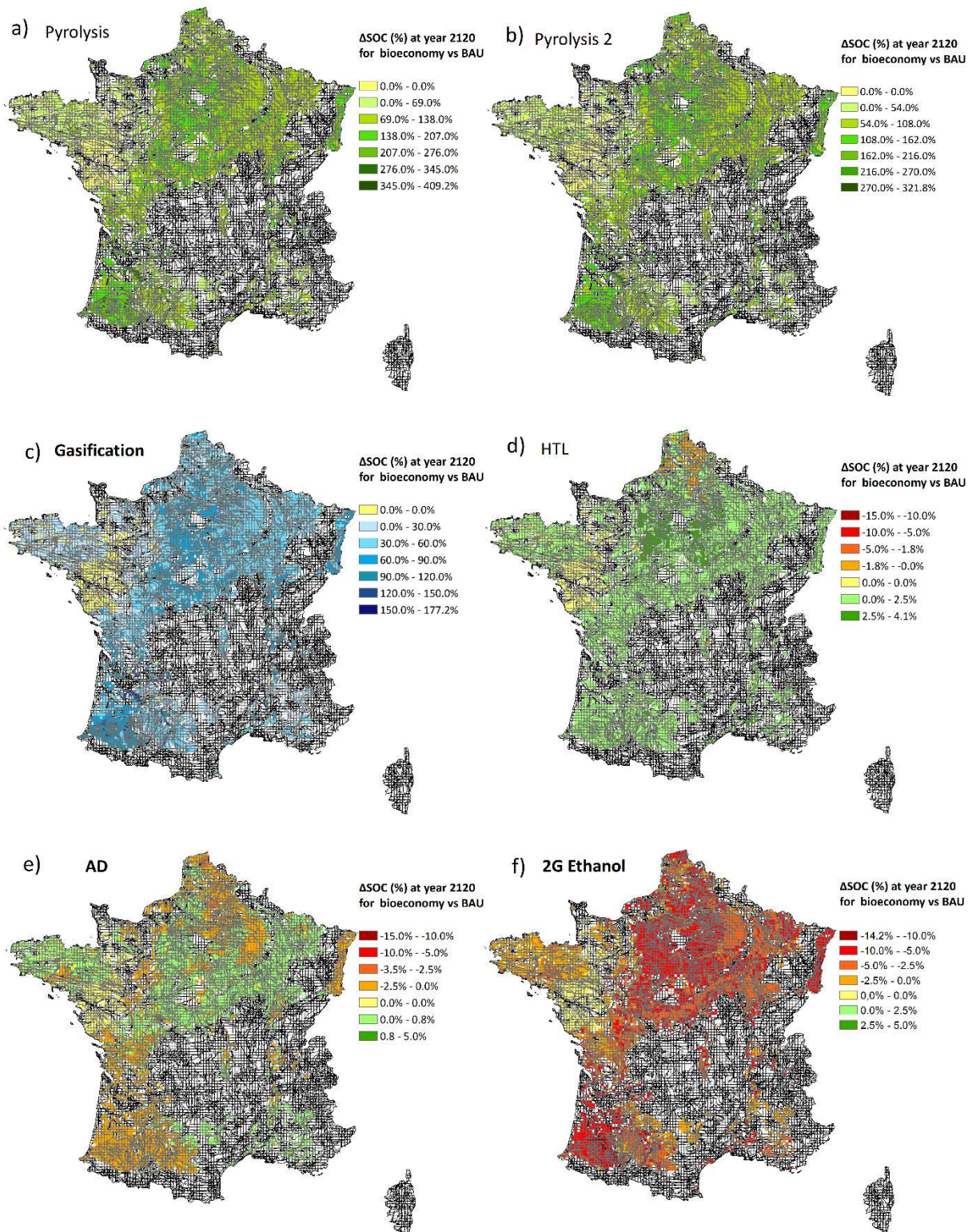
550 If all the harvestable crop residues are exported for pyrolysis or gasification, but only 50
551 t C ha⁻¹ are regularly recycled to the soils throughout the 100 years to avoid the toxic
552 effects of excessive char application, no SOC decreases are observed as a result, on all
553 the APCU.



554

555 Fig 3. Predicted long-term soil organic carbon (SOC) stocks for the BAU scenario at
556 year 2120

557



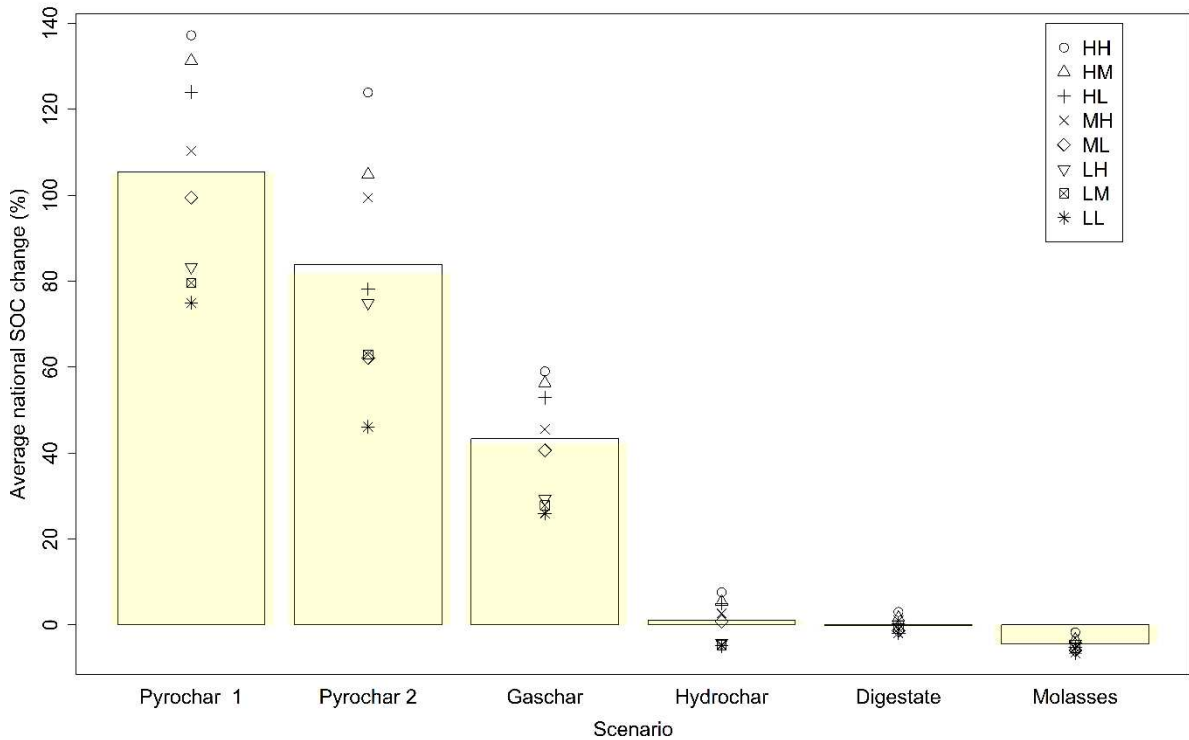
558

559 Fig 4. Spatially explicit soil organic carbon (SOC) stocks relative to the BAU scenario

560 (year 2120) if the available harvestable crop residues are used for bioeconomy

561 ($\Delta\text{SOC}_{\text{bio-base}} \%$) a) Pyrolysis (with C_s pool of AMG only; default), b) pyrolysis (with

562 C_A and C_S pool of AMG; sensitivity), c) gasification, d) HTL, e) anaerobic digestion, f)
 563 lignocellulosic ethanol. White grids were not included in the simulations.



564
 565 Fig 5. Sensitivity analysis describing a combination of low (L), mean (M), and high (H)
 566 C_c and C_r values for each bioeconomy scenario, with an extra scenario for pyrolysis
 567 (Pyrochar2) considering an alternative method to partition the recalcitrant fractions into
 568 SOC pools in AMG. The bars show the MM (C_c+C_r) value while yellow shades
 569 represent the average of all 9 points (SOC at year 2120; in comparison to the BAU) for
 570 the different C_c and C_r combinations in a given scenario.

571 **Table 2.** National 100 y SOC changes from the BAU to the bioeconomy ($\Delta\text{SOC}_{\text{bio-BAU}}$),
 572 in total Mt C and %, at an exporting rate of 100%, at year 2120. Values in % are
 573 provided as national averages of all APCUs.

Bioeconomy scenarios	Total national	Min ^d	Max ^d	Average national	σ^c	Min ^d	Max ^d
----------------------	----------------	------------------	------------------	------------------	------------	------------------	------------------

	$\Delta\text{SOC}_{\text{bio-BAU}^{\text{b}}}$			$\Delta\text{SOC}_{\text{bio-BAU}^{\text{e}}}$			
	(Mt C)			(%)			
BAU ^a	-17.8	-0.1	0.1	-2.2	14.8	-27.0	84.9
Pyrolysis	774.2	0.0 ^f	0.5	105.5	69.3	0.1	409.2
Gasification	315.6	0.0 ^f	0.2	43.3	29.3	0.1	177.2
HTL	8.9	0.0 ^f	0.0 ^f	1.1	0.8	-1.8	4.1
AD	-0.8	-0.0 ^f	0.0 ^f	-0.1	0.4	-3.5	0.7
2G Ethanol	-34.9	-0.0 ^f	0.0 ^f	-4.4	2.9	-14.2	-0.0 ^f

574 ^aBAU scenario corresponds to ΔSOC_{0-100} .

575 ^bSum of all the modeled APCUs

576 ^cStandard deviation

577 ^dMinimum and maximum $\Delta\text{SOC}_{\text{bio-BAU}}$ reported over all APCU

578 ^eAverage SOC change for all the modeled APCUs

579 ^fValue is not zero. More decimals included in Table SI2.2

580 4. DISCUSSION

581 4.1 Long term spatially-explicit co-products potential for SOC stocks

582 The business as usual (BAU) scenario reflecting current practices predicted a slight
583 average decrease (2% for 100 years) of topsoil organic C in the simulated areas, which
584 is consistent with the potential prolongation of average decreases in SOC stocks
585 observed over the past decades in temperate croplands in France, Belgium, and
586 Germany (Clivot et al., 2019; Goidts and van Wesemael, 2007; Meersmans et al., 2011;
587 Steinmann et al., 2016). The simulated decrease is, however, lower than that of 14%
588 obtained by Riggers et al. (2021) in German croplands with a multi-model ensemble for

589 the same climate projection (RCP 4.5) and unchanged (current) C inputs for the 2014-
590 2099 period. The BAU scenario predicted SOC losses in around 63% of all simulated
591 areas (Fig. 3), which is in line with the trends observed in Launay et al. (2021), where
592 SOC decreases on 55% of the simulated areas (STICS model) were observed after 30
593 years. The regional differences observed can be explained by the influence of the initial
594 SOC stocks, climate, soil, and cropping system characteristics.

595 Results differed considerably among the recalcitrance groups (high and low) because
596 the adapted AMG allocates the recalcitrant C as inert for the highly-recalcitrant
597 coproducts, whereas it is allocated to the decomposable active pool for the less
598 recalcitrant coproducts. The steady state normally faced in the active pool is never
599 attained in the stable one, allowing the high recalcitrant products to continue building
600 up SOC stocks over the long-term.

601 In a C-neutral harvesting context, 100% of the harvestable crop residues can be
602 exported for bio-oil or syngas production by pyrolysis or gasification, respectively.
603 Pyrolysis results do compare to those of previous studies. For instance, Lefebvre et al.
604 (2020) reported a 127% SOC increase in 20 years in sugarcane fields by replacing
605 sugarcane bagasse and trash with the biochar produced. Woolf and Lehmann (2012)
606 found that the export of 50% of maize residues for biochar production, with the
607 subsequent addition of biochar to soils, can increase the SOC stocks by 30-60% over
608 100 y.

609 The AD scenario projected a negligible SOC stock increase (up to 0.7%) in 50% of the
610 modeled areas and small SOC losses (up to 4%) in the remaining 40% (the remaining
611 10% being areas where crop residues are already exported for other uses). Evidence
612 suggests that anaerobic digestion does not modify the characteristics of the biomass
613 stable C remaining in the digestate (Möller, 2015), thus the long-term effect on SOC

614 stocks is often not significant. This was also reported in (Thomsen et al., 2013). Bodilis
615 et al. (2015) observed a slight decrease in the SOC stocks after digestate application in
616 French croplands, as compared to undigested biomass using AMG. On the contrary,
617 Mondini et al. (2018) reported a 2-fold SOC increment after digestate application on
618 Italian lands, compared to undigested crop residues using a modified version of RothC.

619 The difference between the raw and digested residual biomass lies in the labile C
620 fraction. The removal of the labile fraction reduces CO₂ emissions from digestate
621 compared to the raw feedstock. Besides C, bioavailable nutrients are concentrated in
622 digestate, often in a form that is more assimilable for plants, which makes it an
623 attractive fertilizer (Wentzel et al., 2015). Using digestate as fertilizer can offset the
624 emissions incurred by mineral fertilizer production and application (Reibel, 2018),
625 though excessive application could increase N emissions (ADEME et al., 2018). Areas
626 depicting SOC decreases should therefore be analyzed in detail to determine whether
627 other benefits (energy and nutrient recovery) are worth taking the risk of losing soil C.

628 The SOC stocks decreased in all the APCUs in the 2GEtOH scenario, which reflects the
629 changed lignin condensation of the biomass exerted by the chemical and enzymatic
630 treatments, allowing the soil microorganisms to decompose the coproducts at a faster
631 rate (Bera et al., 2019; Cayuela et al., 2014, 2010). It is associated with increased
632 microbial activity, which may improve fertility and plant growth (Alotaibi and
633 Schoenau, 2011). Nevertheless, soil application of molasses has been associated with
634 negative impacts on the soil characteristics (e.g., increased salinity and electrical
635 conductivity) and increased GHG emissions in comparison to untreated biomass (Bera
636 et al., 2019; Cayuela et al., 2010). Our results suggest not exchanging the crop residues
637 provision to soils with bioethanol coproducts if the objective is to prevent SOC losses.

638 More research is required to understand the recalcitrance properties and C content of
639 bioethanol coproducts and harness its potential as a soil amendment.

640 *4.2 Crop residues potential for bioeconomy*

641 In France, it is suggested to limit the harvest of cereal straw to leave a share of 41-96%
642 of the technically harvestable residues on the soil to preserve its agronomic functions
643 (France Agrimer, 2020). Similarly, ADEME (2018) determined that by 2050, only 21%
644 of crop residues could be mobilized for the specific needs of biogas production due to
645 agronomical soil functions and issues related to competitive use. Our results suggest
646 that these thresholds may be too stringent for a C-neutral harvesting context, even for
647 anaerobic digestion, where a 75% harvest (and return) rate imply SOC losses below 1%
648 in 37.5% of the areas (maximum loss of 2.6%, in 2.5% of the areas).

649 In fact, considering the results of this study, the harvest potential is 100% (of the
650 technically harvestable feedstock not already used), unless the residues are to be used
651 for bioethanol (0% removal). If to be conservative, we consider export rates of 0% only
652 in the areas where SOC losses are observed with anaerobic digestion and HTL, a
653 reduction of the corresponding crop residue potential of 80% and 3% would be
654 observed, respectively (based on 2021, where the non-exported harvestable crop
655 residues totaled 30.4 Mt dry matter). Comparing this with the potential resulting from
656 applying a generic 68.5% limit (middle of the above range suggested for France) of
657 residues to be left on land, it involves that between 4 (anaerobic digestion) and 11
658 (pyrolysis, gasification) Mt dry matter of additional crop residues are obtained by
659 applying our framework. This corresponds to 149 – 279 PJ y⁻¹ (for a low heating value
660 of 17.5 GJ t⁻¹ DM), the equivalent of the gross electricity generation in Greece and
661 Austria, respectively (BP, 2021).

662 Current French cropping systems must increase the C inputs by 42% on average to
663 reach the 4‰ target (Martin et al., 2021), while recent works predict a required increase
664 of 283% for Germany (Riggers et al., 2021). However, a decreasing SOC stocks trend
665 under a BAU scenario has been identified in this work and others (Launay et al., 2021;
666 Martin et al., 2021). In this context, the management of crop residues, allowing to
667 increase SOC stocks as in the biochar scenarios (pyrochar, gaschar, and hydrochar) and
668 partially in the digestate scenario, are alternatives towards the 4‰ goals.

669 *4.3 Strengths and limitations*

670 The scarcity and high variability of data regarding the coproducts C recalcitrance and
671 the challenge of representing long-term effects on real environments based on short-
672 term laboratory studies require caution in the analysis of the results. The main
673 conclusions do not regard the absolute values predicted but the trends related to the
674 sensitivity of the model to the parameters. We tested a wide range of plausible values
675 for the key parameters, so the conclusions drawn for each technology can provide
676 insightful decision support with regards to the crop residues' potential for bioeconomy.
677 Our results partially show the bioeconomy cause-effect link between the usage of the
678 crop residues and their exporting potentials, with different long-term SOC stocks
679 predictions among scenarios. Using coproducts as EOMs inputs to the soil are expected
680 to modify soil physical, chemical, and biological characteristics in diverse ways. These
681 soil changes can be i) altered net primary production (NPP) due to changes in the
682 amount and quality of input C and nutrients, ii) addition of extra organic compounds to
683 the soils, iii) soil microbiota adaptation to utilize the C in the coproducts (this C being
684 structurally different to the one in plant residues) (Hansen et al., 2017; Oldfield et al.,
685 2019). An excessive application of bioeconomy coproducts may alter soil functions
686 which could, in turn, have some environmental impacts. Moreover, the C in the raw

687 biomass is readily available while in the stabilized or recalcitrant matter the C may be
688 unavailable for microorganisms, which could affect soil functioning and fertility. The
689 SA demonstrated that the 100% of the crop residues can be exported to increase the
690 bioeconomy provision while at the same time restraining the possible negative effects of
691 biochar, by limiting the application, without affecting the SOC stocks.

692 Other limitations can be identified in the adapted model and the case studied herein.
693 Changes in soil fertility induced by the coproducts addition were not considered, as well
694 as the potential changes in soil structure and quality (Drosg et al., 2015; Joseph et al.,
695 2021) due to limitations of the model. Besides, nitrogen dynamics (i.e., nitrate leaching
696 and NH₃ emissions) and atmospheric emissions were not evaluated. It was beyond the
697 scope of this work to analyze the overall life cycle effects of the different bioeconomy
698 strategies (i.e., accounting for the substituted energy and products by the main
699 bioeconomy products), here focusing on SOC changes only. Similarly, how to prioritize
700 the distribution of each specific crop residue to each bioeconomy technology. These
701 considerations, however, need to be assessed in future studies to have a holistic
702 understanding of the environmental impacts of exporting crop residues for each
703 technology.

704 The fine granularity of the simulation units assesses the differences among the French
705 croplands, predicting spatially explicit SOC evolutions under each bioeconomy
706 scenario. This approach allows locating areas where coproducts application can build up
707 SOC stocks. Thus, the model can be used to provide advice for resources management
708 for bioeconomy development in specific locations. The framework developed and the
709 modeling approach can be replicated for other regions at different scales, even with less
710 specific granularity, to evaluate the development of crop-based bioeconomy
711 technologies.

712 The future climate trajectory followed the RCP4.5, however, results may vary for
713 different future climate trajectories. In fact, Mondini et al. (2018) modeled the SOC
714 evolution of Italian croplands amended with eight different EOMs under 12 different
715 climate scenarios, reporting a coefficient of variation ranging from 1.2 to 4.3%. The
716 present study considers unchanged cropping systems and crop yields throughout the 100
717 years. The impact of this hypothesis could be challenged in future works by e.g., using
718 ADEME et al. (2018) projections of cropping systems in France, namely one complying
719 with the Factor 4 initiative, and another prolonging the current trends. Factor 4, a
720 national strategy that aims to divide GHG emissions by a factor of 4 by 2050, envisions
721 better agricultural practices and less livestock while the current trends would lead to
722 higher yields for grass, cereal-, and oleaginous crops. These changes in the cropping
723 systems may affect the SOC dynamics and the ability to export crop residues.

724 We assumed that all cover crops are maintained on soils and all temporary grasslands
725 are exported, while currently ca. 50% of cover crops and 11% of temporary grasslands
726 are being collected at a national scale for anaerobic digestion (ADEME et al., 2018).
727 This surplus provision of digested feedstock may improve the results obtained for the
728 AD scenario. Moreover, we only considered the changes in recalcitrance for the crop
729 residues digested and not for the co-substrate used. Around 50% of the simulation units
730 involve the presence of manure besides other organic amendments, which could be co-
731 digested, resulting in C inputs decrease but C recalcitrance improvements. Nevertheless,
732 this effect is expected to be of minor importance, in the light of previous works (e.g.,
733 Thomsen et al., 2013).

734 Finally, it should be noted that the SOC losses observed for hydrochar, digestate, and
735 molasses, could be compensated if coupled with other strategies, such as i)
736 redistribution of coproduct from areas showing increased SOC stocks, ii) introduction

737 of specific cover crops, iii) changes in farming management, iv) mix of bioeconomy
738 coproducts return. This was, however, beyond the study scope.

739 **CONCLUSIONS**

740 This study demonstrated that to maintain long-term SOC stocks, the harvesting potential
741 of crop residues is influenced by the process for which the biomass is destined and is
742 spatially explicit. The partial return of the crop residues C to soils, as stabilized
743 coproducts, was shown to maintain and even increase SOC stocks, in comparison to the
744 levels achieved by just leaving the residues on soils, allowing to provide a greater
745 amount of feedstock to bioeconomy. The study thus confirmed that current practices
746 blindly limiting the potential of crop residues to a stringent threshold unfairly deprive
747 the bioeconomy of an important amount of biomass.

748 Pyrochar and gaschar were shown, when used as soil C input in exchange for crop
749 residues, to increase SOC stocks in all the French croplands modeled. The HTL
750 scenario predicted SOC stocks increases for 88% of the areas, with a slight loss for the
751 croplands located in the North. The results also indicated that minor SOC gains can be
752 expected through exchanging raw residues for digestate, but only in 50% of the areas,
753 while slight losses were observed on the remaining areas. On the other hand, exporting
754 C from crop residues to be compensated with molasses return was shown to lead to
755 clear losses of SOC stocks in all areas.

756 By adapting the soil carbon model AMG to consider the recalcitrance of returned
757 bioeconomy coproducts, this study provides an operational tool that can guide, for any
758 region, future decisions on the use of crop residues for bioeconomy. However, more
759 research is required regarding recalcitrance, especially of bioethanol coproducts and

760 gasification char, for which studies are scarce and the understanding of the C stability
761 and MRT effects on SOC evolution remain an issue.

762 **ACKNOWLEDGEMENTS**

763 This work was carried out within the framework of the research project Cambioscop
764 (<https://cambioscop.cnrs.fr>), partly financed by the French National Research Agency,
765 Programme Investissement d’Avenir (ANR-17-MGPA-0006) and Region Occitanie
766 (18015981). C. Andrade was additionally funded by the French Embassy in Ecuador
767 under the Project “Fonds de Solidarité pour Projets Innovants” (FSPI).

768 Authors are grateful to Camille Launay for providing the initial data and help with our
769 questions, Serguei Sokol for helping with data manipulation in R, and Julie Constantin
770 and Olivier Therond for initiating the collaboration and data share from the INRAE
771 4p1000 project.

772 **DATA AVAILABILITY STATEMENT**

773 The data that support the findings of this study are openly available in “TBI - Toulouse
774 Biotechnology Institute - T21018” at
775 <https://doi.org/10.48531/JBRU.CALMIP/WYWKIQ>.

776 **REFERENCES**

777 4p1000 [WWW Document], n.d. . L’Initiative internationale “4 pour 1000” Les Sols
778 pour la Sécurité Alimentaire et le Climat. URL <https://www.4p1000.org>
779 ADEME, GrDF, GRTgaz, 2018. Un mix de gaz 100% renouvelable en 2050. Étude de
780 faisabilité technico-économique, Horizons. ADEME, GRDF, GRTgaz.

781 Alotaibi, K.D., Schoenau, J.J., 2011. Enzymatic activity and microbial biomass in soil
782 amended with biofuel production byproducts. *Applied Soil Ecology* 48, 227–
783 235. <https://doi.org/10.1016/j.apsoil.2011.03.002>

784 Andrade, C., Albers, A., Zamora-Ledezma, E., Hamelin, L., 2022. A review on the
785 interplay between bioeconomy and soil organic carbon stocks maintenance.
786 **PREPRINT** (version 1) available at Research Square.
787 <https://doi.org/10.21203/rs.3.rs-1447842/v1>

788 Andriulo, A., Mary, B., Guerif, J., 1999. Modelling soil carbon dynamics with various
789 cropping sequences on the rolling pampas. *Agronomie* 19, 365–377.
790 <https://doi.org/10.1051/agro:19990504>

791 Archontoulis, S.V., Huber, I., Miguez, F.E., Thorburn, P.J., Rogovska, N., Laird, D.A.,
792 2016. A model for mechanistic and system assessments of biochar effects on
793 soils and crops and trade-offs. *GCB Bioenergy* 8, 1028–1045.
794 <https://doi.org/10.1111/gcbb.12314>

795 Bai, X., Huang, Y., Ren, W., Coyne, M., Jacinthe, P., Tao, B., Hui, D., Yang, J.,
796 Matocha, C., 2019. Responses of soil carbon sequestration to climate-smart
797 agriculture practices: A meta-analysis. *Glob Change Biol* 25, 2591–2606.
798 <https://doi.org/10.1111/gcb.14658>

799 Bera, T., Vardanyan, L., Inglett, K.S., Reddy, K.R., O’Connor, G.A., Erickson, J.E.,
800 Wilkie, A.C., 2019. Influence of select bioenergy by-products on soil carbon and
801 microbial activity: A laboratory study. *Science of The Total Environment* 653,
802 1354–1363. <https://doi.org/10.1016/j.scitotenv.2018.10.237>

803 Blanco-Canqui, H., 2013. Crop Residue Removal for Bioenergy Reduces Soil Carbon
804 Pools: How Can We Offset Carbon Losses? *Bioenerg. Res.* 14.

805 Bodilis, A.-M., Trochard, R., Lechat, G., Airiau, A., Lambert, L., Hruschka, S., 2015.
806 Impact de l'introduction d'unités de méthanisation à la ferme sur le bilan
807 humique des sols. Analyse sur 10 exploitations agricoles de la région Pays de la
808 Loire. Fourrages.

809 Bolinder, M.A., Janzen, H.H., Gregorich, E.G., Angers, D.A., VandenBygaart, A.J.,
810 2007. An approach for estimating net primary productivity and annual carbon
811 inputs to soil for common agricultural crops in Canada. *Agriculture, Ecosystems*
812 *& Environment* 118, 29–42. <https://doi.org/10.1016/j.agee.2006.05.013>

813 Bonten, L.T.C., Elferink, E.V., Zwart, K., 2014. Tool to assess effects of bio-energy on
814 nutrient losses and soil organic matter 22.

815 BP, 2021. *Statistical Review of World Energy 2021*.

816 Cayuela, M.L., Kuikman, P., Bakker, R., van Groenigen, J.W., 2014. Tracking C and N
817 dynamics and stabilization in soil amended with wheat residue and its
818 corresponding bioethanol by-product: a ¹³C/ ¹⁵N study. *GCB Bioenergy* 6,
819 499–508. <https://doi.org/10.1111/gcbb.12102>

820 Cayuela, M.L., Oenema, O., Kuikman, P.J., Bakker, R.R., Van Groenigen, J.W., 2010.
821 Bioenergy by-products as soil amendments? Implications for carbon
822 sequestration and greenhouse gas emissions: C and N dynamics from bioenergy
823 by-products in soil. *GCB Bioenergy* no-no. [https://doi.org/10.1111/j.1757-](https://doi.org/10.1111/j.1757-1707.2010.01055.x)
824 [1707.2010.01055.x](https://doi.org/10.1111/j.1757-1707.2010.01055.x)

825 Chen, D., Rojas, M., Samset, B.H., Cobb, K., Diongue-Niang, A., Edwards, P., Emori,
826 S., Faria, S.H., Hawkins, E., Hope, P., Huybrechts, P., Meinshausen, M.,
827 Mustafa, S.K., Plattner, G.-K., Treguier, A.M., 2021. Framing, Context, and
828 Methods., in: *Climate Change 2021: The Physical Science Basis. Contribution*

829 of Working Group I to the Sixth Assessment Report of the Intergovernmental
830 Panel on Climate Change. IPCC.

831 Clivot, H., Mouny, J.-C., Duparque, A., Dinh, J.-L., Denoroy, P., Houot, S., Vertès, F.,
832 Trochard, R., Bouthier, A., Sagot, S., Mary, B., 2019. Modeling soil organic
833 carbon evolution in long-term arable experiments with AMG model.
834 Environmental Modelling & Software 118, 99–113.
835 <https://doi.org/10.1016/j.envsoft.2019.04.004>

836 DRIAS, Météo-France, CERFACS, IPSL, 2013. CNRM-CERFACS-CM5/CNRM-
837 ALADIN63-RCP4.5 [WWW Document]. DRIAS les futurs du climat. URL
838 <http://www.drias-climat.fr/commande> (accessed 9.1.20).

839 Drogg, B., Fuchs, W., Seadi, T.A., Madsen, M., Linke, B., 2015. Nutrient Recovery by
840 Biogas Digestate Processing (No. IEA Bioenergy Task 37). IEA Bioenergy.

841 Durand, Y., Brun, E., Guyomarc'H, G., Lesaffre, B., 1993. A meteorological estimation
842 of relevant parameters for snow models 7.

843 Farina, R., Sándor, R., Abdalla, M., Álvaro-Fuentes, J., Bechini, L., Bolinder, M.A.,
844 Brilli, L., Chenu, C., Clivot, H., Migliorati, M.D.A., Bene, C.D., Dorich, C.D.,
845 Ehrhardt, F., Ferchaud, F., Fitton, N., Francaviglia, R., Franko, U., Giltrap, D.L.,
846 Grant, B.B., Guenet, B., Harrison, M.T., Kirschbaum, M.U.F., Kuka, K.,
847 Kulmala, L., Liski, J., McGrath, M.J., Meier, E., Menichetti, L., Moyano, F.,
848 Nendel, C., Recous, S., Reibold, N., Shepherd, A., Smith, W.N., Smith, P.,
849 Soussana, J.-F., Stella, T., Taghizadeh-Toosi, A., Tsutsikh, E., Bellocchi, G.,
850 2020. Ensemble modelling, uncertainty and robust predictions of organic carbon
851 in long-term bare-fallow soils 25.

852 Fischer, G., Prieler, S., van Velthuisen, H., Berndes, G., Faaij, A., Londo, M., de Wit,
853 M., 2010. Biofuel production potentials in Europe: Sustainable use of cultivated

854 land and pastures, Part II: Land use scenarios. *Biomass and Bioenergy* 34, 173–
855 187. <https://doi.org/10.1016/j.biombioe.2009.07.009>

856 France Agrimer, 2020. L'Observatoire National des Ressources en Biomasse.
857 Évaluation des ressources agricoles et agroalimentaires disponibles en France –
858 édition 2020. Agrimer.

859 Goidts, E., van Wesemael, B., 2007. Regional assessment of soil organic carbon
860 changes under agriculture in Southern Belgium (1955–2005). *Geoderma* 141,
861 341–354. <https://doi.org/10.1016/j.geoderma.2007.06.013>

862 Graux, A.-I., Resmond, R., Casellas, E., Delaby, L., Faverdin, P., Le Bas, C., Ripoche,
863 D., Ruget, F., Théron, O., Vertès, F., Peyraud, J.-L., 2020. High-resolution
864 assessment of French grassland dry matter and nitrogen yields. *European Journal*
865 *of Agronomy* 112, 125952. <https://doi.org/10.1016/j.eja.2019.125952>

866 Haase, M., Rösch, C., Ketzer, D., 2016. GIS-based assessment of sustainable crop
867 residue potentials in European regions. *Biomass and Bioenergy* 86, 156–171.
868 <https://doi.org/10.1016/j.biombioe.2016.01.020>

869 Hamelin, L., Borzęcka, M., Kozak, M., Pudełko, R., 2019. A spatial approach to
870 bioeconomy: Quantifying the residual biomass potential in the EU-27.
871 *Renewable and Sustainable Energy Reviews* 100, 127–142.
872 <https://doi.org/10.1016/j.rser.2018.10.017>

873 Hamelin, L., Naroznova, I., Wenzel, H., 2014. Environmental consequences of different
874 carbon alternatives for increased manure-based biogas. *Applied Energy* 114,
875 774–782. <https://doi.org/10.1016/j.apenergy.2013.09.033>

876 Han, L., Sun, K., Yang, Y., Xia, X., Li, F., Yang, Z., Xing, B., 2020. Biochar's stability
877 and effect on the content, composition and turnover of soil organic carbon.
878 *Geoderma* 364, 114184. <https://doi.org/10.1016/j.geoderma.2020.114184>

879 Hansen, J.H., Hamelin, L., Taghizadeh-Toosi, A., Olesen, J.E., Wenzel, H., 2020.
880 Agricultural residues bioenergy potential that sustain soil carbon depends on
881 energy conversion pathways 12.

882 Hansen, V., Müller-Stöver, D., Imparato, V., Krogh, P.H., Jensen, L.S., Dolmer, A.,
883 Hauggaard-Nielsen, H., 2017. The effects of straw or straw-derived gasification
884 biochar applications on soil quality and crop productivity: A farm case study.
885 Journal of Environmental Management 186, 88–95.
886 <https://doi.org/10.1016/j.jenvman.2016.10.041>

887 He, S., Boom, J., van der Gaast, R., Seshan, K., 2018. Hydro-pyrolysis of
888 lignocellulosic biomass over alumina supported Platinum, Mo₂C and WC
889 catalysts. Frontiers of Chemical Science and Engineering 12, 155–161.
890 <https://doi.org/10.1007/s11705-017-1655-x>

891 IPCC, 2019. 2019 Refinement to the 2006 IPCC Guidelines for National Greenhouse
892 Gas Inventories - Appendix4: Method for Estimating the Change in Mineral Soil
893 Organic Carbon Stocks from Biochar Amendments: Basis for Future
894 Methodological Development. IPCC.

895 Ippolito, J.A., Cui, L., Kammann, C., Wrage-Mönnig, N., Estavillo, J.M., Fuertes-
896 Mendizabal, T., Cayuela, M.L., Sigua, G., Novak, J., Spokas, K., Borchard, N.,
897 2020. Feedstock choice, pyrolysis temperature and type influence biochar
898 characteristics: a comprehensive meta-data analysis review. Biochar 2, 421–438.
899 <https://doi.org/10.1007/s42773-020-00067-x>

900 Jamagne, M., Hardy, R., King, D., 1995. La base de données géographique des sols de
901 France. Étude et Gestion des Sols 16.

902 Joseph, S., Cowie, A.L., Van Zwieten, L., Bolan, N., Budai, A., Buss, W., Cayuela,
903 M.L., Graber, E.R., Ippolito, J.A., Kuzyakov, Y., Luo, Y., Ok, Y.S.,

904 Palansooriya, K.N., Shepherd, J., Stephens, S., Weng, Z. (Han), Lehmann, J.,
905 2021. How biochar works, and when it doesn't: A review of mechanisms
906 controlling soil and plant responses to biochar. GCB Bioenergy gcb.12885.
907 <https://doi.org/10.1111/gcbb.12885>

908 Karan, S.K., Hamelin, L., 2021. Crop residues may be a key feedstock to bioeconomy
909 but how reliable are current estimation methods? Resources, Conservation and
910 Recycling 164, 105211. <https://doi.org/10.1016/j.resconrec.2020.105211>

911 Keel, S.G., Leifeld, J., Mayer, J., Taghizadeh-Toosi, A., Olesen, J.E., 2017. Large
912 uncertainty in soil carbon modelling related to method of calculation of plant
913 carbon input in agricultural systems: Uncertainty in soil carbon modelling. Eur J
914 Soil Sci 68, 953–963. <https://doi.org/10.1111/ejss.12454>

915 Lafargue, I., 2013. Enquête pratiques culturelles grandes cultures et prairies 2011.
916 Application d'intrants sur maïs grain: quelles évolutions en 2011?. Ministry of
917 Agriculture, Agri-Food and Forestry, France.

918 Launay, C., Constantin, J., Chlebowski, F., Houot, S., Graux, A., Klumpp, K., Martin,
919 R., Mary, B., Pellerin, S., Therond, O., 2021. Estimating the carbon storage
920 potential and greenhouse gas emissions of French arable cropland using high-
921 resolution modeling. Glob. Change Biol. 27, 1645–1661.
922 <https://doi.org/10.1111/gcb.15512>

923 Leenhardt, D., Therond, O., Mignolet, C., 2012. Quelle représentation des systèmes de
924 culture pour la gestion de l'eau sur un grand territoire ?
925 <http://www.agronomie.asso.fr/?id=56>.

926 Lefebvre, D., Williams, A., Meersmans, J., Kirk, G.J.D., Sohi, S., Goglio, P., Smith, P.,
927 2020. Modelling the potential for soil carbon sequestration using biochar from

928 sugarcane residues in Brazil. *Sci Rep* 10, 19479. [https://doi.org/10.1038/s41598-](https://doi.org/10.1038/s41598-020-76470-y)
929 [020-76470-y](https://doi.org/10.1038/s41598-020-76470-y)

930 Lehmann, J., Abiven, S., Kleber, M., Pan, G., Singh, B.P., Sohi, S.P., Zimmerman,
931 A.R., 2015. Persistence of biochar in soil, in: *Biochar for Environmental*
932 *Management*. p. 48.

933 Lehmann, J., Hansel, C.M., Kaiser, C., Kleber, M., Maher, K., Manzoni, S., Nunan, N.,
934 Reichstein, M., Schimel, J.P., Torn, M.S., Wieder, W.R., Kögel-Knabner, I.,
935 2020. Persistence of soil organic carbon caused by functional complexity. *Nat.*
936 *Geosci.* 13, 529–534. <https://doi.org/10.1038/s41561-020-0612-3>

937 Levavasseur, F., Martin, P., Scheurer, O., 2015. *RPG Explorer*, notice d'utilisation 114.

938 Levavasseur, F., Mary, B., Christensen, B.T., Duparque, A., Ferchaud, F., Kätterer, T.,
939 Lagrange, H., Montenach, D., Resseguier, C., Houot, S., 2020. The simple AMG
940 model accurately simulates organic carbon storage in soils after repeated
941 application of exogenous organic matter 15.

942 Lychuk, T.E., Izaurralde, R.C., Hill, R.L., McGill, W.B., Williams, J.R., 2015. Biochar
943 as a global change adaptation: predicting biochar impacts on crop productivity
944 and soil quality for a tropical soil with the Environmental Policy Integrated
945 Climate (EPIC) model. *Mitig Adapt Strateg Glob Change* 20, 1437–1458.
946 <https://doi.org/10.1007/s11027-014-9554-7>

947 Malghani, S., Juschke, E., Baumert, J., Thuille, A., Antonietti, M., Trumbore, S.,
948 Gleixner, G., 2015. Carbon sequestration potential of hydrothermal
949 carbonization char (hydrochar) in two contrasting soils; results of a 1-year field
950 study. *Biology and Fertility of Soils* 51, 123–134.
951 <https://doi.org/10.1007/s00374-014-0980-1>

952 Martin, M.P., Dimassi, B., Román Dobarco, M., Guenet, B., Arrouays, D., Angers,
953 D.A., Blache, F., Huard, F., Soussana, J., Pellerin, S., 2021. Feasibility of the 4
954 per 1000 aspirational target for soil carbon: A case study for France. *Glob*
955 *Change Biol* 27, 2458–2477. <https://doi.org/10.1111/gcb.15547>

956 Mathanker, A., Das, S., Pudasainee, D., Khan, M., Kumar, A., Gupta, R., 2021. A
957 Review of Hydrothermal Liquefaction of Biomass for Biofuels Production with
958 a Special Focus on the Effect of Process Parameters, Co-Solvents, and
959 Extraction Solvents. *Energies* 14, 4916. <https://doi.org/10.3390/en14164916>

960 Meersmans, J., Van Wesemael, B., Goidts, E., Van Molle, M., De Baets, S., De Ridder,
961 F., 2011. Spatial analysis of soil organic carbon evolution in Belgian croplands
962 and grasslands, 1960-2006: Spatial Analysis of soil organic carbon evolution.
963 *Global Change Biology* 17, 466–479. [https://doi.org/10.1111/j.1365-](https://doi.org/10.1111/j.1365-2486.2010.02183.x)
964 [2486.2010.02183.x](https://doi.org/10.1111/j.1365-2486.2010.02183.x)

965 Molino, A., Larocca, V., Chianese, S., Musmarra, D., 2018. Biofuels Production by
966 Biomass Gasification: A Review. *Energies* 11, 811.
967 <https://doi.org/10.3390/en11040811>

968 Möller, K., 2015. Effects of anaerobic digestion on soil carbon and nitrogen turnover, N
969 emissions, and soil biological activity. A review. *Agron. Sustain. Dev.* 35,
970 1021–1041. <https://doi.org/10.1007/s13593-015-0284-3>

971 Mondini, C., Cayuela, M.L., Sinicco, T., Fornasier, F., Galvez, A., Sánchez-Monedero,
972 M.A., 2018. Soil C Storage Potential of Exogenous Organic Matter at Regional
973 Level (Italy) Under Climate Change Simulated by RothC Model Modified for
974 Amended Soils. *Front. Environ. Sci.* 6, 144.
975 <https://doi.org/10.3389/fenvs.2018.00144>

976 Mondini, C., Cayuela, M.L., Sinicco, T., Fornasier, F., Galvez, A., Sánchez-Monedero,
977 M.A., 2017. Modification of the RothC model to simulate soil C mineralization
978 of exogenous organic matter (preprint). *Biogeochemistry: Soils*.
979 <https://doi.org/10.5194/bg-2016-551>

980 Monforti, F., Lugato, E., Motola, V., Bodis, K., Scarlat, N., Dallemand, J.F., 2015.
981 Optimal energy use of agricultural crop residues preserving soil organic carbon
982 stocks in Europe. *Renewable and Sustainable Energy Reviews* 44, 519–529.
983 <https://doi.org/10.1016/j.rser.2014.12.033>

984 Morais, T.G., Teixeira, R.F.M., Domingos, T., n.d. Detailed global modelling of soil
985 organic carbon in cropland, grassland and forest soils 27.

986 Mulder, V.L., Lacoste, M., Richer-de-Forges, A.C., Martin, M.P., Arrouays, D., 2016.
987 National versus global modelling the 3D distribution of soil organic carbon in
988 mainland France. *Geoderma* 263, 16–34.
989 <https://doi.org/10.1016/j.geoderma.2015.08.035>

990 Oldfield, E.E., Bradford, M.A., Wood, S.A., 2019. Global meta-analysis of the
991 relationship between soil organic matter and crop yields. *SOIL* 5, 15–32.
992 <https://doi.org/10.5194/soil-5-15-2019>

993 Panoutsou, C., Kyriakos, M., 2021. Sustainable biomass availability in the EU, to 2050.
994 Concawe.

995 R Core Team, 2021. R: A language and environment for statistical computing. R
996 Foundation for Statistical Computing, Viena, Austria.

997 Reibel, A., 2018. Valorisation agricole des digestats : Quels impacts sur les cultures, le
998 sol et l'environnement ? Revue de littérature, La Méthanisation en Provence-
999 Alpes-Cote d'Azur. GERE, ADEME.

1000 Riggers, C., Poeplau, C., Don, A., Frühauf, C., Dechow, R., 2021. How much carbon
1001 input is required to preserve or increase projected soil organic carbon stocks in
1002 German croplands under climate change? *Plant Soil* 460, 417–433.
1003 <https://doi.org/10.1007/s11104-020-04806-8>

1004 Sadh, P.K., Duhan, S., Duhan, J.S., 2018. Agro-industrial wastes and their utilization
1005 using solid state fermentation: a review. *Bioresour. Bioprocess.* 5, 1.
1006 <https://doi.org/10.1186/s40643-017-0187-z>

1007 Saffih-Hdadi, K., Mary, B., 2008. Modeling consequences of straw residues export on
1008 soil organic carbon. *Soil Biology and Biochemistry* 40, 594–607.
1009 <https://doi.org/10.1016/j.soilbio.2007.08.022>

1010 Sarker, S., Lamb, J.J., Hjelme, D.R., Lien, K.M., 2019. A Review of the Role of Critical
1011 Parameters in the Design and Operation of Biogas Production Plants. *Applied*
1012 *Sciences* 9, 1915. <https://doi.org/10.3390/app9091915>

1013 Scarlat, N., Fahl, F., Lugato, E., Monforti-Ferrario, F., Dallemand, J.F., 2019. Integrated
1014 and spatially explicit assessment of sustainable crop residues potential in
1015 Europe. *Biomass and Bioenergy* 122, 257–269.
1016 <https://doi.org/10.1016/j.biombioe.2019.01.021>

1017 Smith, P., Soussana, J.-F., Angers, D., Schipper, L., Chenu, C., Rasse, D.P., Batjes,
1018 N.H., van Egmond, F., McNeill, S., Kuhnert, M., Arias-Navarro, C., Olesen,
1019 J.E., Chirinda, N., Fornara, D., Wollenberg, E., Álvaro-Fuentes, J., Sanz-
1020 Cobena, A., Klumpp, K., 2020. How to measure, report and verify soil carbon
1021 change to realize the potential of soil carbon sequestration for atmospheric
1022 greenhouse gas removal. *Global Change Biology* 26, 219–241.
1023 <https://doi.org/10.1111/gcb.14815>

- 1024 Steinmann, T., Welp, G., Holbeck, B., Amelung, W., 2016. Long-term development of
1025 organic carbon contents in arable soil of North Rhine–Westphalia, Germany,
1026 1979–2015. *European Journal of Soil Science* 67, 616–623.
1027 <https://doi.org/10.1111/ejss.12376>
- 1028 Swain, M.R., Singh, A., Sharma, A.K., Tuli, D.K., 2019. Chapter 11 - Bioethanol
1029 Production From Rice- and Wheat Straw: An Overview, in: *Bioethanol*
1030 Production from Food Crops. Sustainable Sources, Interventions, and
1031 Challenges. Academic Press, p. 19.
- 1032 Thomsen, I.K., Olesen, J.E., Møller, H.B., Sørensen, P., Christensen, B.T., 2013.
1033 Carbon dynamics and retention in soil after anaerobic digestion of dairy cattle
1034 feed and faeces. *Soil Biology and Biochemistry* 58, 82–87.
1035 <https://doi.org/10.1016/j.soilbio.2012.11.006>
- 1036 Tonini, D., Hamelin, L., Astrup, T.F., 2016. Environmental implications of the use of
1037 agro-industrial residues for biorefineries: application of a deterministic model
1038 for indirect land-use changes. *GCB Bioenergy* 8, 690–706.
1039 <https://doi.org/10.1111/gcbb.12290>
- 1040 Ventura, M., Alberti, G., Panzacchi, P., Vedove, G.D., Miglietta, F., Tonon, G., 2019.
1041 Biochar mineralization and priming effect in a poplar short rotation coppice
1042 from a 3-year field experiment. *Biol Fertil Soils* 55, 67–78.
1043 <https://doi.org/10.1007/s00374-018-1329-y>
- 1044 Wang, J., Xiong, Z., Kuzyakov, Y., 2016. Biochar stability in soil: meta-analysis of
1045 decomposition and priming effects. *GCB Bioenergy* 8, 512–523.
1046 <https://doi.org/10.1111/gcbb.12266>
- 1047 Watson, J., Wang, T., Si, B., Chen, W.-T., Aierzhati, A., Zhang, Y., 2020. Valorization
1048 of hydrothermal liquefaction aqueous phase: pathways towards commercial

1049 viability. *Progress in Energy and Combustion Science* 77, 100819.
1050 <https://doi.org/10.1016/j.peccs.2019.100819>

1051 Watson, J., Zhang, Y., Si, B., Chen, W.-T., de Souza, R., 2018. Gasification of
1052 biowaste: A critical review and outlooks. *Renewable and Sustainable Energy*
1053 *Reviews* 83, 1–17. <https://doi.org/10.1016/j.rser.2017.10.003>

1054 Wentzel, S., Schmidt, R., Piepho, H.-P., Semmler-Busch, U., Joergensen, R.G., 2015.
1055 Response of soil fertility indices to long-term application of biogas and raw
1056 slurry under organic farming. *Applied Soil Ecology* 96, 99–107.
1057 <https://doi.org/10.1016/j.apsoil.2015.06.015>

1058 Wietschel, L., Messmann, L., Thorenz, A., Tuma, A., 2021. Environmental benefits of
1059 large-scale second-generation bioethanol production in the EU: An integrated
1060 supply chain network optimization and life cycle assessment approach. *Journal*
1061 *of Industrial Ecology* 25, 677–692. <https://doi.org/10.1111/jiec.13083>

1062 Witing, F., Prays, N., O’Keeffe, S., Gründling, R., Gebel, M., Kurzer, H.-J., Daniel-
1063 Gromke, J., Franko, U., 2018. Biogas production and changes in soil carbon
1064 input - A regional analysis. *Geoderma* 320, 105–114.
1065 <https://doi.org/10.1016/j.geoderma.2018.01.030>

1066 Woolf, D., Amonette, J.E., Street-Perrott, F.A., Lehmann, J., Joseph, S., 2010.
1067 Sustainable biochar to mitigate global climate change. *Nat Commun* 1, 56.
1068 <https://doi.org/10.1038/ncomms1053>

1069 Woolf, D., Lehmann, J., 2012. Modelling the long-term response to positive and
1070 negative priming of soil organic carbon by black carbon 13.

1071 Woolf, D., Lehmann, J., Ogle, S., Kishimoto-Mo, A.W., McConkey, B., Baldock, J.,
1072 2021. Greenhouse Gas Inventory Model for Biochar Additions to Soil. *Environ.*
1073 *Sci. Technol.* *acs.est.1c02425*. <https://doi.org/10.1021/acs.est.1c02425>

1074 Zhang, Q., Xiao, J., Xue, J., Zhang, L., 2020. Quantifying the Effects of Biochar
1075 Application on Greenhouse Gas Emissions from Agricultural Soils: A Global
1076 Meta-Analysis. *Sustainability* 12, 3436. <https://doi.org/10.3390/su12083436>
1077 Zimmerman, A., Gao, B., 2013. The Stability of Biochar in the Environment, in:
1078 Ladygina, N., Rineau, F. (Eds.), *Biochar and Soil Biota*. CRC Press, pp. 1–40.
1079 <https://doi.org/10.1201/b14585-2>
1080 Zimmerman, A.R., 2010. Abiotic and Microbial Oxidation of Laboratory-Produced
1081 Black Carbon (Biochar). *Environ. Sci. Technol.* 44, 1295–1301.
1082 <https://doi.org/10.1021/es903140c>
1083

Supplementary Files

This is a list of supplementary files associated with this preprint. Click to download.

- [Andradeetal.2022.Thecropresidueconundrum.SI1.pdf](#)
- [Andradeetal.CaseModelingSI2.xlsx](#)